4841 Revision 2

A general model for calculating the viscosity of natural iron-bearing silicate melts over a wide range of temperature, pressure, oxygen fugacity and compositions

Xianzhe Duan[1, 2*]

[1]School of Nuclear Resource Engineering, University of South China, Hengyang, Hunan 421001, China

[2]State Key Laboratory of Lithospheric Evolution, Institute of Geology and Geophysics, Chinese Academy of Sciences, Beijing 100029, China

---

[*] Corresponding author (duanxianzhe@126.com , and duanxianzhe@163.com)

ABSTRACT

A new general model that takes into account the pressure and redox state effect is presented to calculate melt viscosities of natural Fe-bearing melts. This new model is applicable to melts that span a wide range of temperatures (from 733 K to 1873 K), pressures (0.001-15 kbar), H_2O content (from 0 wt% to 12.3 wt%), and compositions (from ultramafic, mafic to silicic melts). The accuracy of the model is calculated to be ± 0.23 log units of viscosity, which is within or close to experimental uncertainty. The transport properties, including glass transition temperature and melt fragility, can also be calculated from this model. A spreadsheet to calculate the viscosity is provided in an Electronic Supplement.

Keywords: Melt viscosity; Fe-bearing melts; Oxygen fugacity; Iron oxidation state; Glass transition temperature; Melt fragility; Volcanic eruption

INTRODUCTION

The viscosity of silicate melts is one of the most important physical properties governing magmatic processes such as the generation, migration, degassing, crystallization and eruption of magmas (e.g., Shaw, 1972; Hui and Zhang, 2007; Giordano et al., 2008). It is well known that the main parameters that control the viscosity of melts are temperature and melt composition (including water) (e.g., Shaw, 1963, 1972; Kushiro, 1976, 1978b, 1986; Persikov, 1991; Baker, 1996; Schulze et al., 1996; Stevenson et al., 1996; Richet et al., 1996; Stevenson et al., 1998; Zhang, 1999; Whittington et al., 2000, 2001; Romano et al., 2003;Zhang et al., 2003; Dingwell et al.,1996, 2000, 2004; Hui and Zhang, 2007; Ardia et al., 2008; Hui et al., 2009; Giordano et al., 2003, 2006, 2008; Vetere et al., 2007, 2008; Misiti et al., 2006, 2011; Bartels et al., 2012; Chevrel et al., 2013). In general, the melt viscosity has non-Arrhenius temperature dependence, and can be significantly reduced by H_2O, which is the most abundant fluid in the upper mantle and crust. In addition to temperature and composition effects, the pressure and redox state (i.e., iron oxidation state or oxygen fugacity) may have important effects (Mysen et al., 1980; Liebske et al., 2003; Mysen and Richet, 2005; Ardia et al., 2008; Hui et al., 2009; Bartels et al., 2012). For instance, Mysen et al. (1980) suggested that it was necessary to consider the pressure effect during the magma ascent from upper mantle to Earth surface, and Liebske et al., (2003) reported that the viscosities of dry andesitic melts could decrease by about 1.6 log units with increasing Fe^{2+}/Fe_{tot} from 0.42 to 0.79. In addition, oxygen fugacity controlling the iron oxidation state has been widely recognized to

play an important role in the structure of melt, thereby significantly affecting melt viscosity (Cukierman and Uhlmann, 1974; Liebske et al., 2003; Mysen and Richet, 2005; Vetere et al., 2008). Due to the importance of viscosity in geological processes, many experiments on the viscosity of melts have been performed over the past half century (e.g., Shaw, 1963; Kushiro, 1986; Persikov, 1991; Toplis et al., 1994; Stevenson et al., 1995; Richet et al., 1996; Giordano et al., 2003b; Liebske et al., 2003, 2005; Vetere et al., 2007, 2008; Chevrel et al., 2013). However, these data are far from sufficient for geological applications over a wide *T-P-X* range of Earth's deep interior due to the inconsistencies within and between the published data sets, particularly at the high *T-P* range where the data are scattered due to the difficulty in experimental technique (Avramov, 2007; Ardia et al., 2008; Hui et al., 2009). Therefore, many researchers have devoted extensive efforts to the modeling of viscosity in melts in order to interpolate between data points or extrapolate beyond the data range (e.g., Shaw 1972; Baker et al., 1996; Richet et al., 1996; Schulze et al., 1996; Scaillat et al., 1996; Hess and Dingwell., 1996; Zhang et al., 2003; Misiti et al., 2006, 2011; Vetere et al., 2006, 2007, 2008; Avramov, 2007; Hui and Zhang, 2007; Giordano et al., 2003, 2006, 2008; Ardia et al., 2008; Hui et al 2009) (see the Electronic Supplement for detail).

In this study, I provide a model in which pressure effect and iron oxidation state effect on viscosity have been taken into account. First, the available data are reviewed in Section 2. The framework of the model is presented in Section 3. Then this model is compared with the experimental data with the previous models (Section 4), where evaluation of the model accuracy was performed by the root-mean-square-error (abbreviated as RMSE, hereafter) between the measured and calculated viscosity data, which is defined as follows:

$$RMSE = \sqrt{\frac{\sum_{i=1}^{n}\left(\log_{10}\eta_{cal}{}^{i} - \log_{10}\eta_{\exp}{}^{i}\right)^2}{n}} \qquad (1)$$

where $\eta_{cal}{}^{i}$ and $\eta_{\exp}{}^{i}$ are the ith calculated and measured viscosity data in Pa s, respectively; n is the number of the data. As can be seen from Eqn. (1), RMSE can be used to measure the goodness of prediction of certain model of interest. Section 5 contains a discussion of the viscosity behavior of natural melts, with the complicated effects exerted by temperature, pressure, melt composition (including water), and redox state.

The new model can predict viscosities of various natural Fe-bearing melts from 733 K to 1873 K and from 0.001 kbar to 15 kbar with accuracy within or close to experimental data (e.g., RMSE of 0.23 log units).

REVIEW OF VISCOSITY DATA

Over the last half century, experimental scientists have carried out extensive measurements of viscosity of a large variety of natural Fe-bearing silicate melts (from ultra-mafic, mafic and to silicic) over a large temperature-pressure range (Fig. 1).

In constructing the literature database for this model, the data used for calibration meet the following minimal criteria: (1) experiments must be on natural silicate melt compositions, (2) complete compositions of melts must have been determined, (3) the redox state (i.e., iron oxidation state or oxygen fugacity) should be known, (4) the melts need not to experience a large variation in the iron oxidation state or the crystallization during the viscosity measurements. Among the experimental measurements for Fe-bearing melts (Fig. 1), some

fulfill these requirements (Shaw, 1963; Kushiro, 1986; Persikov, 1991; Toplis et al., 1994; Stevenson et al., 1995; Richet et al., 1996; Giordano et al., 2003b; Liebske et al., 2003, 2005; Vetere et al., 2007, 2008；Chevrel et al., 2013), with the following exceptions: (1) several data points of Giordano et al. (2003b) measured for basaltic melts at temperatures above 1670 K are inconsistent with that of Toplis et al. (1994) with a deviation more than 1 log units; (2) several data points of Liebske et al. (2003) collected during heating are not consistent with their data collected during cooling; (3) the data points of Chevrel et al. (2013) where the melt compositions used were distinctly different from those of natural melts. These small amounts of experimental data are not used for parameterization.

The experimental data (Labeled as "Data_redox_state_known", hereafter) of this database compiled for anhydrous to hydrous Fe-bearing melts covers more than 14.5 orders of magnitude of viscosity ($10^{-1.72}$-$10^{12.8}$Pa s), showing near-Arrhenian to non-Arrhenian temperature dependence, includes more than 220 measurements on more than 20 melt compositions spanning the *T-P* range of 733-2523 K and 0.001-130 kbar. In this database, Liebske et al. (2005) provide the only data for pressures above 15 kbar (i.e., 28-130 kbar). This data set was not used for calibration, but instead for a check of the model predictability. Two sets of viscosity on andesitic melts (Liebske et al., 2003) and shoshonitic melts (Vetere et al., 2007) are also not included in the parameterization, but are also chosen to test whether this model can predict data not in the fit (Table 1).

Some data (Labeled as "Data_redox_state_unknown", hereafter) with unknown redox states (Neuville et al., 1993; Stevenson et al., 1996; Alidibirov et al., 1997; Gottsman et al., 2002; Romano et al., 2003; Misiti et al., 2006, 2011) are chosen for checking the

predictability of this model in the case where the redox state effect is not under consideration, compared with the H-Z model (Hui and Zhang, 2007) and G-R-D model (Giordano et al., 2008) that are mostly popularly used.

MODEL FORMULATION AND PARAMETERIZATION

Integrating the strengths of the previous models, the effects of melt composition and iron oxidation on melt viscosity were evaluated in this study by a parameter named VSM, which is a modified version of the SM parameter of Giordano et al. (2003a). SM is a 'network modifiers' parameter as the molar percentage oxide sum, as defined as the following equation (Eqn. (2)), and was used as a compositional parameter to calculate anhydrous multi-component melt viscosity.

$$SM = \sum(Na_2O + K_2O + CaO + MgO + MnO + FeO_{tot} / 2) \qquad (2)$$

where FeO_{tot} is the total iron content.

However, iron can exist in both divalent and trivalent states in melts. Divalent iron can act as a network modifier, while trivalent iron can act as a network former, like Si^{4+}, Ti^{4+}, Al^{3+}, P^{5+} (Persikov et al., 1990; Dingwell et al., 1993; Toplis and Dingwell, 1996; Ottonello et al., 2001; Moretti, 2005; Mysen and Richet, 2005). I therefore modified the SM expression by distinguishing between the two different valences and roles of iron in silicate melt, treating all ferric iron as a network former and all ferrous iron as a network modifier. If the iron oxidation state is not given, the method of Moretti (2005) is used to calculate it under the given *T-P-X-*fO_2 condition. There are some various empirical forms have been proposed to

quantitatively calculate the iron oxidation state as a function of oxygen fugacity, pressure, temperature and compositions of the melt (Sack et al., 1980; Kilinc et al., 1983; Kress and Carmichael, 1991). Later work attempted to include the effect of water (Moore et al., 1995), while the most recent attempt to predict iron oxidation state including the effect of water has been presented by Moretti (2005), which is the extension of Ottonello et al. (2001). The method of Moretti (2005) for the determination of the iron oxidation state is mainly based on the following three assumptions: (1) iron oxidation state is dominantly controlled by five variables (oxygen fugacity, pressure, temperature, melt composition, water); (2) FeO can produce Fe^{2+} and O^{2-} (Flood and Forland, 1947) and H_2O can be dissociated to H^+ and O^{2-} (Fraser, 1975, 1977); (3) Fe_2O_3 behaves as an amphoteric oxide in the Lux-Flood acid-base acceptation, i.e., Fe_2O_3 in the melt can be double dissociated into Fe^{3+} (basic dissociation) and FeO^{2-} anions (acidic dissociation) (Fraser, 1975, 1977; Ottonello et al., 2001). With the calculated mole fractions of Fe^{2+} and Fe^{3+} in the silicate melt, I replace the total Fe in the SM expression Eq. (2), by the mole fraction of Fe^{2+} and added the oxides such as SiO_2, TiO_2, Al_2O_3, Fe^{3+} and P_2O_5 to the denominator to create the VSM parameter.

$$VSM = \frac{\sum(Na_2O + K_2O + CaO + MgO + MnO + Fe^{2+})}{\sum(SiO_2 + TiO_2 + Al_2O_3 + Fe^{3+} + P_2O_5)} \qquad (3)$$

where Fe^{2+} and Fe^{3+} are the relative proportion of ferrous and ferric iron in the total iron, respectively; VSM represents the enrichment of non-bridging oxygen atoms in the melt system. Non-bridging oxygen is related to the depolymerization of melts, which in turn affects the amount of free oxygen in the melts and thus influences the viscosity (Mysen and Richet, 2005).

The VSM value calculated from the anhydrous melt composition was chosen to

175 characterize the melts. A single value parameter of melt composition, NBO/T, was also used
176 by Giordano et al. (2003a) to model the viscosity of anhydrous melts, while the researchers
177 also used the SM to describe the melt composition in their models (e.g., Giordano et al.,
178 2003a, 2006). The use of individual oxides in models creates additional fitting parameters,
179 typically more than 10; additional model parameters results in better fitting of the model to
180 the calibration data. However, models with many parameters can sometimes produce
181 inaccurate interpolations and extrapolation (Kenny and McCoach, 2003). Because of this
182 possibility, the VSM parameter is used to characterize anhydrous melt composition and
183 produces a model that provides accurate predictions of viscosity for most common,
184 Fe-bearing melts.

185 In spite of the importance of water in affecting the structure and properties of silicate
186 melts, the relative abundance of the species of it dissolved in melts both as hydroxyl groups
187 and molecular species, appears to be a complex function of at least temperature and melt
188 composition that currently defy accurate modeling (e.g., Silver and Stolper, 1989; Silver et al.,
189 1990; Zhang, 1999; Mysen and Richet, 2005). For the purpose of creating a simple-to-use
190 model, a method is needed to reflect the influence of water on the viscosity that does not rely
191 upon experimental measurements of the water species in the melts, but yet adequately
192 quantifies the effect of water on the viscosity. After considering many different methods, I
193 incorporated the effect of water by the product of VSM and the mole fraction of total water in
194 the melts.

195 Based on the Vogel-Fulcher-Tammann equation (abbreviated as VFT equation, hereafter)
196 which expresses the non-Arrhenian temperature dependence of viscosity (Vogel, 1921;

197 Fulcher, 1925; Tammann and Hesse, 1926; Russell et al., 2003), the following equation (Eqn.
198 (4)), which most accurately reproduces the data, is proposed in this study:

$$\log\eta = A + \frac{B}{T-C}$$
$$A = a$$
$$B = b_1 + b_2\ln(JB)$$
$$C = c_1 + c_2\ln(JC)$$
$$JB = b_3^{\,2} + VSM(b_4^{\,2}VSM + 2b_3b_4 + b_4X_{H_2O} + b_4b_5P) + X_{H_2O}(2b_3 + X_{H_2O} + b_5P + b_4VSM) + P(2b_3b_5 + b_5^{\,2}P + b_4b_5VSM + b_5X_{H_2O}) \quad (4)$$
$$JC = c_3^{\,2} + VSM(c_4^{\,2}VSM + 2c_3c_4 + c_4X_{H_2O} + c_4c_5P) + X_{H_2O}(2c_3 + X_{H_2O} + c_5P + c_4VSM) + P(2c_3c_5 + c_5^{\,2}P + c_4c_5VSM + c_5X_{H_2O})$$

199

200 where T is in Kelvin, P is in kbar; η is viscosity in Pa s; The values of parameters a, b_1-b_5
201 and c_1-c_5 are listed in Table 2. X_{H2O} is molar fraction of the volatile (H_2O) in melts on a single
202 oxygen basis as defined below (Eqn. (5)) (Stolper, 1982; Zhang, 1999).

203 $$X_{H_2O} = (C_{H_2O} / M_{H_2O}) / (C_{H_2O} / M_{H_2O} + (100 - C_{H_2O}) / W) \quad (5)$$

204 where C_{H2O} and M_{H2O} are mass percent and mass per mole of H_2O, respectively, W is the mass
205 of dry melt per mole of oxygen.

206 As can be found in Eqn. (4), the viscosity is modeled as the combination of the affects of
207 temperature, pressure, redox state, anhydrous melt composition, and water concentration.

208 The R^2 value and RMSE for fitting the data used for the calibration of this model (Table
209 1) is 0.996 and 0.23, respectively, indicating that this model reproduces the data within or
210 close to the experimental accuracy. The common value of parameter A indicates that the
211 viscosity at infinite temperature based on the model for various Fe-bearing melts (log
212 η_∞=-4.75, negligible compositional dependence) is close to the value of log η_∞=-4.31$\pm$0.74

obtained by Russell et al. (2003) to be the optimized viscosity limit for silicate melts. With these parameters, the viscosity of natural Fe-bearing silicate melts including anhydrous and hydrous iron-bearing melts can be calculated.

VALIDATION OF THE MODEL

More than 10 viscosity models were chosen for comparison in this study (Table 3, which also lists the references denoted by the following model abbreviations).

Fig. 2 (a-c) shows the comparisons of the calculated viscosities with this model, H-Z model and the G-R-D model, and the experimental data, including those with known (Data_redox_state_known) and unknown redox states (Data_redox_state_unknown). It should be noted that for proper comparison, the outliers of the H-Z and G-R-D model (Toplis et al., 1994; Richet et al., 1996) were not used in the comparison. In addition, where the information on redox state is absent (Fig. 2a), the contents of FeO and Fe_2O_3 were arbitrarily calculated with the assumption that half of the total iron FeO_{tot} (wt%) is FeO (wt%) and the other half is Fe_2O_3 (wt%); this was also done in cases where the Fe^{2+}/Fe^{3+} ratios were known (Data_redox_state_known). Fig. 3 compares the predictions of this model with the experimental data with known redox states (Data_redox_state_known). The experimental measurements of iron oxidation state are taken as inputs for the calculation of viscosities with this model. Only the experimental data within the stated *T-P-X* ranges of models are used in Figs. 2-3.

The viscosities calculated from this model are comparable to the H-Z and G-R-D models, and can be applicable in the condition where the redox state effect is unknown (Fig. 2). However, the accuracy of previous models for calculating the viscosity of Fe-bearing melts, especially for high iron-bearing melts (e.g., basalt, andesite) (e.g., Toplis et al., 1994; Richet et al., 1996), can be much improved by incorporating redox state effect, as can be seen from Fig. 3.

The viscosity model from this study can reproduce the experimental data used in the calibration with a standard deviation of 0.23 log units, and those not used in the calibration within 0.28 log units. These results illustrate the robustness of the model within and beyond its calibration range.

Fig. 4 shows the good prediction of this model at high pressures ($P \geqq 1$ kbar), with a remarkable accuracy (RMSE=0.27). However, additional experimental data at higher pressures ($P > 15$ kbar) is needed for better constraining the model.

Table 3 shows the results of comparisons between the experimental data (Data_redox_state_known) and that calculated by this model, and those of previous general models (e.g., S-B-W model; H-Z model; G-R-D model) and the other specific models in comparison. It can be seen by comparing the different values of RMSE that the model of this study gives better results than the previous models in predicting viscosities of various natural Fe-bearing melts over a wide temperature and pressure range. The S-B-W model produces an RMSE of 0.77 log units when compared to experimentally determined melt viscosities. Moreover, the S-B-W model is only applicable to viscosities below 10^5 Pa s. The comparison between the measurements and the predictions of H-Z model produces the RMSE of 0.7 log

256 units, whereas the comparisons of G-R-D model viscosity predictions with the measurements
257 on various melts yield the RMSE of 0.68 log units. The calculated viscosities of various
258 natural Fe-bearing melts with this model is about 0.5 log units more accurate than previous
259 general models (H-Z model; G-R-D model). In addition, the H-Z and G-R-D models include
260 more parameters (37 and 18, respectively) than this model (11) (Table 3), which may result in
261 less accurate interpolations and extrapolations (e.g., Kenny and McCoach, 2003). The
262 relatively large deviations yielded by both H-Z model and G-R-D model for Fe-bearing melts
263 probably reflects that they did not account for the iron redox state.

264 On the other hand, this model gives comparable results to other models except for
265 shoshonitic melts (Vetere et al., 2007), where the standard deviation of this model is 0.40 log
266 units, which is 0.23 log units higher than the V-B-M model (RMSE of 0.17 log units).
267 However, the V-B-M model used the Vetere et al (2007) data for calibration, whereas in the
268 model presented here the data used as a check.

269 This model is based on the data for Fe-bearing melts, and should not be used for Fe-free
270 melts, where the H-Z or G-R-D models are recommended. In addition, this model is best
271 recommended for Fe-bearing melts with well characterized redox states. If the oxygen
272 fugacity rather than iron oxidation state is given, it is recommended to evaluate the iron
273 oxidation state prior to the determination of melt viscosity according to the method of Moretti
274 (2005), which is the most recent attempt to quantitatively calculate the iron oxidation state as
275 a function of oxygen fugacity, pressure, temperature, melt composition and H_2O. The
276 calculation can be done with the files found in the Electronic Supplement. If neither iron
277 oxidation state nor oxygen fugacity are known, the total FeO content (FeO_{tot}, wt%) could be

278 split equally between FeO (wt%) and Fe_2O_3 (wt%) for the calculation of melt viscosity.

279

280 ## DISCUSSION

281

282 ### The temperature, pressure and compositional effects on the viscosity

283

284 While some workers (e.g., Bottinga and Weill, 1972; Shaw, 1972) in the earlier studies
285 assumed an Arrhenius temperature dependence of melt viscosity, it has been most widely
286 accepted that the viscosities of silicate melts have non-Arrhenian temperature dependence,
287 and that this dependence is more pronounced in the lower temperature range (e.g., Mysen,
288 1988; Richet and Bottinga, 1995; Hess and Dingwell, 1996; Zhang et al., 2003; Mysen and
289 Richet, 2005; Vetere et al., 2006, 2007, 2008; Misiti et al., 2006, 2011; Hui and Zhang, 2007;
290 Giordano et al., 2008).

291 The important role that the pressure plays in viscosity was not recognized until 1970s.
292 The pressure dependence of viscosity is complicated, and is still subject of debate (e.g.,
293 Kushiro, 1976, 1978a; Scarfe et al., 1979, 1987; Mysen et al., 1980; Brearley et al., 1986;
294 Gupta, 1987; Bottinga and Richet, 1995; Richet et al., 1996; Schulze et al., 1996, 1999; Mori
295 et al., 2000; Behrens and Schulze, 2003; Reid et al., 2003; Liebske et al., 2003, 2005; Poe et
296 al., 2006; Ardia et al., 2008; Vetere et al., 2006, 2008; Hui et al., 2009; Del Gaudio and
297 Behrens, 2009; Bartels et al., 2012). Kushiro (1976) found that the viscosity of albitic melts
298 could decrease by 1 log units from 5 kbar to 24 kbar in the high temperature range. Kushiro
299 (1978a) found a similar decrease of viscosity for jadeite with increasing pressure. Gupta

(1987) also reported a negative pressure dependence of viscosity in some synthetic melts (e.g., Na_2O-$3SiO_2$; Na_2O-Al_2O_3-$4SiO_2$; K_2O-MgO-$5SiO_2$; Na_2O-Al_2O_3-$6SiO_2$). Some workers (e.g., Kushiro, 1976, 1978a; Mori et al., 2000; Ardia et al., 2008) interpreted this remarkable decrease as the consequence of the coordination change of Al in melts, i.e., from four- to six-fold or the decrease in the T-O-T (T=Si, Al) angle weakening the silicate network. Other works (e.g., Scarfe et al., 1979, 1987; Mysen et al., 1980; Brearley et al., 1986; Bottinga and Richet, 1995; Schulze et al., 1999; Behrens and Schulze, 2003; Del Gaudio and Behrens, 2009) suggested that the variation in the viscosity was mainly related to the degree of melt polymerization. For instance, Scarfe et al. (1979) noted that the viscosity of highly polymerized melts exhibited a negative pressure dependence, whereas the less highly polymerize melts showed a positive pressure dependence. Scarfe et al. (1987) found that in the low viscosity range, a positive pressure effect existed in some silicate melts with NBO/T>1, like diopside, whereas most silicate melts with NBO/T<1, such as andesite, tholeiitic basalt, were characterized by a negative pressure effect. On the other hand, in the high viscosity range, the negative pressure effect on viscosity was also found for polymerized melts such as albitic melts (Schulze et al., 1999; Behrens and Schulze, 2003; Del Gaudio and Behrens, 2009). Del Gaudio and Behrens (2009) observed that at low temperature, the pressure effect appeared to be more important than at high temperature. Nevertheless, Reid et al. (2003) reported an “anomalous’ pressure dependence of viscosity for diopside, showing that the viscosity increased from 35 kbar to a maximum at 100 kbar and then decreased at higher pressure. A pressure dependence similar to that reported by Reid et al. (2003) was also observed in Liebske et al. (2005), who reported that the viscosity results for peridotite had a

maximum at the pressure (i.e., 85 kbar). This viscosity behavior with pressure was explained to be likely associated with structure changes of melt that occur upon compression (Reid et al., 2003; Liebske et al., 2005; Poe et al., 2006). A minor effect of pressure on viscosity of synthetic rhyolitic to more feldspaitic melts (Schulze et al., 1996; Bartels et al., 2012), but also of iron-free andesite and iron-bearing andesite has been reported (Richet et al., 1996; Liebske et al., 2003; Vetere et al., 2006, 2008). Liebske et al. (2003) found the variation in viscosity of iron-free andesite was less than 0.3 orders of magnitude in the pressure range from 1 kbar to 3 kbar. Vetere et al. (2006) observed no significant dependence of viscosity in hydrous iron-free andesite on pressure in the range of 0.001-5 kbar at high temperature. Vetere et al. (2008) suggested that pressure had a minor influence for hydrous iron-bearing andesite with high water content ($H_2O \geqq 2.5$ wt%) in the low viscosity range, although these authors stated that they didn't have experimental pairs where only pressures were changing (identical temperature, melt composition and iron redox state). Fig. 5 shows the prediction of this model on the pressure dependence of viscosity at 1473 K and in the 0.001 kbar-10 kbar pressure range, demonstrating that the pressure has a minor effect on iron-bearing andesitic melts with high H_2O content at high temperature, in good agreement with the pressure trend observed by previous studies (e.g., Liebske et al., 2003; Vetere et al., 2006, 2008). However, when the H_2O decreases, the effect of pressure becomes larger, and cannot be ignored. For instance, the viscosity of iron-bearing andesitic melt with 6 wt% H_2O content, decreases by less than 0.4 orders of magnitude with increasing pressure from 0.001 kbar to 3 kbar, but can decrease by about 0.8 orders of magnitude when H_2O content decreases to about 0.1 wt%. A similar pressure trend can also be found at pressures beyond 3 kbar. Therefore, in spite of

344 smaller influence on viscosity relative to temperature, the pressure effect cannot be neglected
345 to model the viscosity in the geologically relevant conditions. This result is consistent with the
346 point suggested by Mysen et al. (1980) that the pressure effect should be taken into account
347 under the condition during the magma ascent from Earth depth to surface.

348 H_2O is of great importance to viscosity because small variation in H_2O content can cause
349 significant changes in viscosity and thus ultimately influence the mechanisms of
350 transportation and eruption of magma (Shaw, 1963; Kushiro, 1978b; Dingwell et al., 1996,
351 2000; Papale, 1999; Whittington et al., 2000, 2001; Zhang et al., 2003; Morizet et al., 2007;
352 Vetere et al., 2007, 2008; Hui et al., 2009; Misiti et al., 2011; Duan, 2014). It is well
353 recognized that H_2O has a significantly negative effect on viscosities of melts, regardless of
354 the melt types, but the viscosity behavior corresponding to H_2O effect has been hotly debated
355 (e.g., Shaw, 1963; Kushiro, 1978b; Davis and Tomozawa, 1996; Dingwell et al., 1996; Zhang,
356 1999;Whittington et al., 2000, 2001; Zhang et al., 2003; Morizet et al., 2007; Misiti et al.,
357 2011). Shaw (1963) found the addition of 1 wt% water could cause the reduction by two
358 orders of magnitude in the viscosity of initially anhydrous rhyolitic melts. Dingwell et al.
359 (1996) reported that the viscosity of haplogranitic melts dropped drastically with the addition
360 of 0.5 wt% of water and then decrease at water contents of 2 wt%. Richet et al. (1996)
361 suggested a strongest decrease of viscosity for andesitic melts at low water. For example, 1
362 wt% H_2O can decrease viscosity by more than 5 orders of magnitude, but a further viscosity
363 decrease by only 2 orders of magnitude with an additional 2.5 wt% H_2O. A similar effect was
364 observed by Whittington et al. (2000, 2001), who found a decrease of viscosity by 3 orders of
365 magnitude resulted from the first addition of 1 wt% of water, but smaller reductions with

366 further additions of water for both trachyte and phonolite at 900 K. Kushiro (1978b) observed
367 a difference in H_2O dependence of viscosity at high temperature and low temperature. For
368 instance, addition of 3.5 wt% H_2O reduces melt viscosity by 7 orders of magnitude at 1 bar
369 and 1000 K, whereas the viscosity is reduced by only 1.5 orders of magnitude with 4.5 wt%
370 H_2O at 1600 K and 15 kbar. Some works (e.g., Shaw, 1963; Davis and Tomozawa, 1996;
371 Zhang, 1999; Dingwell et al., 2000; Whittington et al., 2000, 2001; Morizet et al., 2007;
372 Misiti et al., 2011) reported that the decreased viscosity for a given amount of H_2O was highly
373 dependent on melt composition, e.g., H_2O effect was more pronounced in more polymerized
374 melts. The decrease of viscosity with H_2O may be attributed to the modification of silicate
375 network and thus depolymerization of melt resulted from the reactions between H_2O and
376 melts (Davis and Tomozawa, 1996; Zhang, 1999)
377
378 **The influence of redox state on the viscosity**
379
380 Although some studies (e.g., Moore et al., 1995; Richet et al., 1996) suggested no effect
381 of redox state on melt viscosity, it has been more widely accepted that the redox state plays an
382 important role on melt viscosity (e.g., Cukierman and Uhlmann, 1974; Klein et al., 1983;
383 Mysen, 1988; Dingwell and Virgo, 1988; Mysen and Virgo, 1989; Dingwell, 1991; Neuville et
384 al., 1993; Toplis et al., 1994; Liebske et al., 2003; Dingwell et al., 2004; Hui and Zhang, 2007;
385 Vetere et al., 2008; Giordano et al., 2008). In general, the increase of Fe^{2+}/Fe_{tot} ratio (or
386 decrease of Fe^{3+}/Fe_{tot}) leads to the decrease of viscosity (Klein et al., 1983; Dingwell, 1989;
387 Neuville et al., 1993). A decrease in viscosity by 0.81 log units on average when Fe^{2+}/Fe_{tot}

388 increases from about 0 to 0.77 was found for the system Na-Si-Fe-O (composition NS4F40),
389 whereas a decrease by 0.34 log units was found for $NaFeSi_2O_6$ melt when the Fe^{2+}/Fe_{tot} ratio
390 increases from 0.08 to 0.82 (Mysen and Virgo, 1989). Liebske et al. (2003) reported that
391 viscosity of dry andesitic melts could decrease by about 1.6 log units when the Fe^{2+}/Fe_{tot} ratio
392 increases from 0.42 to 0.79 at 1061 K. Dingwell et al. (2004) found the effect of iron
393 oxidation state on melt viscosity is more pronounced at lower temperature than is at higher
394 temperature. Vetere et al. (2008) indicated that changing Fe^{2+}/Fe_{tot} from 0.83 to 0.60 could
395 cause the increase of viscosity of andesitic melts at high temperature ($\geqq$1473K) with low
396 water ($H_2O \leqq 0.1$ wt%) by about 1 log units. The effect of redox state on viscosity of various
397 Fe-bearing melts at 0.001 kbar and 1473 K is shown in Fig. 6a, b, where the oxygen fugacity
398 of each melt corresponds to its iron oxidation state, illustrating that the redox state may exert
399 a significant effect on viscosity. For example, the viscosity of Fe-bearing andesitic melts can
400 increase by about 0.8 log units at 1473 K when increasing the Fe^{3+}/Fe_{tot} ratio from 0.2 to 0.6,
401 where for basaltic melts there is 0.86 log units increase in viscosity for the same variation of
402 iron oxidation state (Fig. 6a). In addition, the viscosities of Fe-bearing basaltic melts,
403 andesitic melts and rhyolitic melts can increase by about 0.5 log units, 0.8 log units and 0.6
404 log units, respectively, at 0.001 kbar and 1473 K when increasing the oxidation state from
405 $\triangle$NNO-2 to $\triangle$NNO+2 (Fig. 6b) (note here: $\triangle$NNO is the oxygen fugacity relative to NNO
406 buffer, see O'Neill, 1987) . Fig. 6c shows the significant effect of oxygen fugacity on the
407 'network modifiers' parameter (VSM) of various Fe-bearing melts under the same *T-P*
408 conditions as described in Fig. 6(a-b). From Fig. 6, it can be found that the oxygen fugacity
409 may substantially affect iron oxidation state and melt polymerization, and thus exert a

410 significant effect on the viscosity.

411

412 **Application of the model**

413

414 This new model can be used for the calculation of other physical properties of silicate
415 melts, such as the glass transition temperature (Tg) and the melt fragility (m). The glass
416 transition represents the transition from a melt to a solid phase, and plays a vital role in
417 volcanic eruptions because the mechanical response of the magma or lava to applied stress at
418 this brittle/ductile transition governs the eruptive behavior (Sato et al., 1992; Gottsmann et al.,
419 2002). Tg is the temperature division between the relaxed liquids and unrelaxed glasses and is
420 defined as follows (Eqn. (6)) (Dingwell and Webb, 1990; Angell, 1991; Plazek and Ngai,
421 1991; Stevenson et al., 1995; Dingwell, 1995; Moynihan, 1995; Webb and Dingwell, 1995;
422 Gottsmann et al., 2002).

423 $$\log\eta\Big|_{T=T_g} = K - \log|q| \qquad (6)$$

424

425 where the K and q are the shift factor and cooling rate, respectively; K may reflect a melt
426 structure influence on the relationship between relaxation time and Tg (Stevenson et al., 1995;
427 Gottsmann et al., 2002). K is treated differently in different works. For example, Gottsmann et
428 al. (2002) and Dingwell et al. (2004) considered it as a function of melt composition, whereas
429 it was treated as a constant in Stevenson et al. (1995). In this study, the method of Gottsmann
430 et al. (2002) is used to calculate Tg as function of cooling rate and silicate melt composition.

431 Melt fragility can be used to measure the degree of deviation of viscosity from an

Arrhenian temperature dependence; strong melts tend to have an Arrhenian behavior, whereas fragile melts show a non-Arrhenian behavior (Plazek and Ngai, 1991). It is clearly defined in Toplis et al., (1997) that the fragility (m) of melts is the gradient of the viscosity trace at the glass transition temperature and can be calculated with Eqn. (7).

$$m = fragility = \left.\frac{d(\log_{10}\eta)}{d(T_g/T)}\right|_{T=T_g} = \frac{B}{T_g(1-C/T_g)^2} \qquad (7)$$

where B and C are the parameters in this model (Eqn. (4)).

Fig. 7a shows the strong effect of H_2O on Tg. The main effect of increased H_2O is to depress values of Tg (Fig. 7a). Model values of Tg decrease sharply with increasing H_2O content (Fig. 7a), which is in agreement with the experimental studies of Giordano et al. (2004a, b). The largest decrease in Tg (145-334 K) is predicted to occur within the first 3 wt% H_2O. Anhydrous melts with Tg values of 893-1125 K have predicted Tg values of 700-725 K at 12 wt% H_2O (Fig. 7a).

Numerous discrepancies exist in the literature on the effect of H_2O on melt fragility, and there is currently no consensus. For example, a negative H_2O dependence of melt fragility in various melts was proposed by some works (e.g., Giordano et al., 2003, 2006, Giordano et al. 2008; Del Gaudio et al., 2007), whereas positive H_2O dependence of melt fragility in some polymerized melts (e.g., rhyolitic melts) was obtained in others (e.g., Hess and Dingwell 1995; Zhang et al., 2003; Malfait et al., 2013). Though the effect of H_2O on melt fragility is not well understood, some researchers (e.g., Kohn, 2000; Zhang et al., 2003; Del Gaudio et al., 2007; Deubener et al., 2008; Di Genova et al., 2013; Malfait and Sanchez-Valle, 2013) interpreted it as the consequence of the variation in the melt structure mainly associated with the

453 dissolution behavior of water in different silicate melts. A negative correlation between the
454 melt fragility and H_2O is predicted by this model (Fig. 7b). This result is consistent with that
455 obtained by Giordano et al. (2003, 2006, 2008) and Del Gaudio et al. (2007). The implication
456 is that dry melt that shows non-Arrhenius behavior tends to become more Arrhenian with
457 increasing H_2O content. Fig. 7b also shows that anhydrous rhyolitic to basaltic melts have
458 fragility values of 28.5-32.7, but their fragility values virtually overlap at about 22 and with
459 12 wt% H_2O. Although the negative relationship between melt fragility and H_2O in rhyolitic
460 melts contrasts with their positive correlation obtained by some works (e.g., Hess and
461 Dingwell 1995; Zhang et al., 2003; Malfait et al., 2013), there is a common consensus that
462 H_2O indeed exerts a significant effect on fragilities of melts, regardless of the melt types,
463 especially under low water condition (Fig. 7b).

464 As described above, the glass transition temperature (Tg) and fragility (m) of degassing
465 melt would significantly increase as a consequence of the decreasing H_2O water during
466 magma ascent, implying that melt becomes more non-Arrhenian in its temperature
467 dependence and that the potential of melt for explosive fragmentation increases, respectively,
468 ultimately resulting in volcanic eruption (Fig. 7) (e.g., Angell, 1991; Plazek and Ngai, 1991;
469 Toplis et al., 1997; Stevenson et al., 1995; Gottsmann et al., 2002; Giordano et al., 2004a, b;
470 Giordano et al., 2008).

471

472 **Implication for the petrogenesis of magmas**

473

474 The viscosities of Fe-bearing melts calculated by this model are almost 0.5 orders of

magnitude higher than those calculated by the previous general models that did not include the Fe oxidation state. The higher viscosities would result in substantially slower ascent velocities of Fe-bearing melts than previously calculated. For example, although the transport rates in dikes are poorly known, a simple model has been proposed for elucidating the rheological relations between the velocity (u) and viscosity of magmas through the volcanic conduits (Eqn. (8)) (Mastin and Ghiorso, 2000; Mastin, 2002; Mastin, 2005):

$$u = -(R^2 / 8\eta)(\partial P / \partial z + \rho g) \quad (8)$$

where u is the average flow velocity, R is the radius of the conduit; η is the viscosity, P is the pressure; z is vertical position (upwards being positive); ρ is density of melt; g is gravitational acceleration. As the value of $(\partial P / \partial z + \rho g)$ is negative in an upward flowing conduit with z positive in the upward direction (Mastin 2005), the velocity of melt shows inversely dependence upon melt viscosity at the given R and $(\partial P / \partial z + \rho g)$. The rates of separation and ascent through dikes of Fe-bearing melts are slower than previously considered possible because of the higher viscosities calculated by this model than previous general models. The concept that the ascent of melt diapirs through the upward flowing conduit relies on the rheology of the deforming region of wall rock immediately surrounding the ascending diapir was proposed by Mahon et al. (1988), which used S-B-W model for calculating melt viscosities prior to the calculations of the rheology of the deformation region. Although the calculation of dispir ascent viscosities was not conducted in this study, substitution into the Mahon et al. (1988) calculations of partially molten wall rock viscosities estimated by this model would decrease diapiric ascent rate, and thus increase the depth of final diapir emplacement.

497 This new general model presented in this work represents significant improvement over
498 previous general models (e.g., H-Z model; G-R-D model) for the prediction of the viscosities
499 of Fe-bearing melts and is in good agreement with measured viscosities. These higher
500 viscosities result in almost a half orders-of-magnitude decreases in the melt-transport
501 processes occurring in the Fe-bearing magmas.
502
503 ***Acknowledgement*** I greatly appreciate Dr. Fidel Costa and two anonymous reviewers for
504 their valuable and constructive suggestions, which greatly contributed to the improvement of
505 this manuscript. I much thank Dr. Fidel Costa for his significant efforts to kindly polish this
506 manuscript at late stage, Dr. Keith Putirka for his kind assistance in the further improvement
507 of this manuscript, Drs. Keith Putirka, Don R Baker, Bjorn Mysen, Alexander Bartels and
508 Kai-Uwe Hess for their insightful comments on this paper at early stage of this manuscript
509 that have done much help to strengthen this manuscript, and Drs. Zhigang Zhang, Chi Zhang,
510 Ming Geng, and Guangjun Guo for their kind help in this work. This research is supported by
511 the Open Project from State Key Laboratory of Lithospheric Evolution, Institute of Geology
512 and Geophysics, Chinese Academy of Sciences.
513
514 **REFERENCES**
515 Angell, C.A. (1991) Relaxation in liquids, polymers and plastic crystals -strong/fragile
516 patterns and problems. Journal of Non-Crystalline Solids, 131-133**,** 13-31.
517 Ardia, P., Giordano, D., and Schmidt, M.W. (2008) A model for the viscosity of rhyolite as a
518 function of H_2O-content and pressure: A calibration based on centrifuge piston cylinder

519 experiments. Geochimica et Cosmochimica Acta, 72, 6103-6123.

520 Avramov, I. (2007) Pressure and temperature dependence of viscosity of glassforming and of
521 geoscientifically relevant systems. Journal of Volcanology and Geothermal Research,
522 160, 165-174.

523 Baker, D. (1996) Granitic melt viscosities: Empirical and configurational entropy models for
524 their calculation. American Mineralogist, 81, 126-134.

525 Bartels, A., Behrens, H., Holtz, F., Schmidt, B.C., Fechtelkord, M., Knipping, J., Crede, L.,
526 Baasner, A., and Pukallus, N. (2012) The effect of fluorine, boron and phosphorus on the
527 viscosity of pegmatite forming melts. Chemical Geology 346, 184-198.

528 Behrens, H., and Schulze, F. (2003) Pressure dependence of melt viscosity in the system
529 $NaAlSi_3O_8$-$CaMgSi_2O_6$. American Mineralogist, 88(8-9), 1351-1363.

530 Bottinga, Y., and Weill, D.F. (1972) The viscosity of magmatic silicate liquids; a model
531 calculation. American Journal of Science, 272, 438-475.

532 Bottinga, Y., and Richet, P. (1995) Silicate melts: The "anomalous" pressure dependence of
533 the viscosity. Geochimica et Cosmochimica Acta, 59(13), 2725-2731.

534 Brearley, M., and Dickinson, J. (1986) Pressure dependence of melt viscosities on the join
535 diopside-albite. Geochimica et Cosmochimica Acta, 50(12), 2563-2570.

536 Chevrel, M.O., Baratoux, D., Hess, K.-U., and Dingwell, D.B. (2013) Viscous flow behavior
537 of tholeiitic and alkaline Fe-rich martian basalts. Geochimica et Cosmochimica Acta, In
538 Press.

539 Cukierman, M., and Uhlmann, D.R. (1974) Effects of iron oxidation state on viscosity, Lunar
540 composition. Journal of Geophysical Research 79, 1594-1598.

Davis, K.M., and Tomozawa, M. (1996) An infrared spectroscopic study of water-related species in the silicate glasses. Journal of Non-Crystalline Solids, 201, 177-198.

Del Gaudio, P., Behrens, H., and Deubener, J. (2007) Viscosity and glass transition temperature of hydrous float glass. Journal of Non-Crystalline Solids, 353(3), 223-236.

Del Gaudio, P., and Behrens, H. (2009) An experimental study on the pressure dependence of viscosity in silicate melts. Journal of Chemical Physics, 131, 044504.

Deubener, J., Helsch, G., Moiseev, A., and Bornhoft, H. (2009) Glasses for solar energy conversion systems. Journal of the European Ceramic Society, 29(7), 1203-1210.

Di Genova, D., Romano, C., Hess, K.-U., Vona, A., Poe, B., Giordano, D., Dingwell, D., and Behrens, H. (2013) The rheology of peralkaline rhyolites from Pantelleria Island. Journal of Volcanology and Geothermal Research, 249, 201-216.

Dingwell, D. (1989) Shear viscosities of ferrosilicate liquids. American Mineralogist, 74, 1038-1044.

Dingwell, D. (1991) Redox viscometry of some Fe-bearing silicate melts. American Mineralogist, 76, 1560-1562.

Dingwell, D., Romano, C., and Hess, K. (1996) The effect of water on the viscosity of a haplogranitic melt under PTX conditions relevant to silicic volcanism. Contributions to Mineralogy and Petrology, 124, 19-28.

Dingwell, D.B., and Virgo, D. (1988) Melt viscosities in the Na_2O-FeO-Fe_2O_3-SiO_2 system and factors controlling the relative viscosities of fully polymerized silicate melts. Geochimica et Cosmochimica Acta, 52, 395-403.

Dingwell, D., Courtial, P., Giordano, D., and Nichols, A. (2004) Viscosity of peridotite liquid.

563 Earth and Planetary Science Letters, 226, 127-138.

564 Dingwell, D., Knoche, R., and Webb, S. (1993) The effect of P_2O_5 on the viscosity of
565 haplogranitic liquid. European Journal of Mineralogy, 5, 133-140.

566 Dingwell, D.B. (1995) Relaxation in silicate melts; some applications. Reviews in Mineralogy
567 and Geochemistry, 32, 21-66.

568 Dingwell, D. B., Hess, K.-U., and Romano, C. (2000) Viscosities of granitic (sensu lato) melts:
569 Influence of the anorthite component. American Mineralogist, 85, 1342-1348.

570 Dingwell, D.B., and Webb, S.L. (1990) Relaxation in silicate melts. European Journal of
571 Mineralogy, 2, 427-449.

572 Duan, X. Z. (2014) A general model for predicting the solubility behavior of H_2O-CO_2 fluids
573 in silicate melts over a wide range of pressure, temperature and compositions.
574 Geochimica et Cosmochimica Acta, 125, 582-609.

575 Flood, H. and Forland, T. (1947) The acidic and basic properties of oxides. Acta Chemical
576 Scand, 1, 592-604.

577 Fraser, D. G. (1975) Activities of trace elements in silicate melt. Geochimica et
578 Cosmochimica Acta, 39, 1525-1530.

579 Fraser, D. G. (1977) Thermodynamic properties of silicate melt. Thermodynamics in Geology,
580 301-325.

581 Fulcher, G.S. (1925) Analysis of recent measurements of the viscosity of glasses. Journal of
582 the American Ceramic Society, 8, 339-355.

583 Giordano, D., and Dingwell, D.B. (2003a) Viscosity of hydrous Etna basalt: implications for
584 Plinian-style basaltic eruptions. Bulletin of Volcanology, 65, 8-14.

585 Giordano, D., and Dingwell, D.B. (2003b) Non-Arrhenian multicomponent melt viscosity: a
586 model. Earth and Planetary Science Letters, 208, 337-349.
587 Giordano, D., Mangiacapra, A., Potuzak, M., Russell, J., Romano, C., Dingwell, D., and Di
588 Muro, A. (2006) An expanded non-Arrhenian model for silicate melt viscosity: A
589 treatment for metaluminous, peraluminous and peralkaline liquids. Chemical Geology,
590 229, 42-56.
591 Giordano, D., Romano, C., Papale, P., and Dingwell, D.B. (2004a) The viscosity of trachytes,
592 and comparison with basalts, phonolites, and rhyolites. Chemical Geology, 213, 49-61.
593 Giordano, D., Romano, C., Dingwell, D., Poe, B., and Behrens, H. (2004b) The combined
594 effects of water and fluorine on the viscosity of silicic magmas. Geochimica et
595 Cosmochimica Acta, 68, 5159-5168.
596 Giordano, D., Russell, J. K., and Dingwell, D.B. (2008) Viscosity of magmatic liquids: A
597 model. Earth and Planetary Science Letters, 271, 123-134.
598 Gottsmann, J., Giordano, D., and Dingwell, D.B. (2002) Predicting shear viscosity during
599 volcanic processes at the glass transition: a calorimetric calibration. Earth and Planetary
600 Science Letters, 198, 417-427.
601 Gupta, P.K. (1987) Negative pressure dependence of viscosity. Journal of the American
602 Ceramic Society, 70(7), C152-C153.
603 Hess, K.U., and Dingwell, D.B. (1996) Viscosities of hydrous leucogranitic melts: A
604 non-Arrhenian model. American Mineralogist, 81, 1297-1300.
605 Hui, H., and Zhang, Y. (2007) Toward a general viscosity equation for natural anhydrous and
606 hydrous silicate melts. Geochimica et Cosmochimica Acta, 71, 403-416.

607 Hui, H., Zhang, Y., Xu, Z., Del Gaudio, P., and Behrens, H. (2009) Pressure dependence of
608 viscosity of rhyolitic melts. Geochimica et Cosmochimica Acta, 73, 3680-3693.
609 Kenny, D.A., and McCoach, D.B. (2003) Effect of the number of variables on measures of fit
610 in structural equation modeling. Structural. Equation. Modeling, 10, 333-351.
611 Klein, L.C., FA sano, B.V., and Wu, J.M. (1983) Viscous flow behavior of four
612 iron-containing silicates with alumina, effects of composition and oxidation condition.
613 Journal of Geophysical Research, 88, A880-A886.
614 Kilinc, A., Carmichael, I.S.E., Rivers, M.L., and Sack, R.O. (1983) The ferric-ferrous ratio of
615 natural silicate liquids equilibrated in air. Contributions to Mineralogy and Petrology,
616 83(1), 136-140.
617 Kushiro, I. (1976) Changes in viscosity and structure of melt of $NaAlSi_2O_6$ composition at
618 high pressures. Journal of Geophysical Research, 81(35), 6347-6350.
619 Kushiro, I. (1978a) Viscosity and structural changes of albite ($NaAlSi_3O_8$) melt at high
620 pressures. Earth and Planetary Science Letters **41**, 87-90.
621 Kushiro, I. (1978b) Density and viscosity of hydrous calc-alkalic andesite magma at high
622 pressre. Carnegie Institute of Washington Year Book **77**, 675-678.
623 Kushiro, I. (1986) Viscosity of partial melts in the upper mantle. Journal of Geophysical
624 Research, 91, 9343-9350.
625 Le Bas, M., Le Maitre, R., Streckeisen, A., and Zanettin, B. (1986) A chemical classification
626 of volcanic rocks based on the total alkali-silica diagram. Journal of Petrology, 27,
627 745-750.
628 Liebske, C., Behrens, H., Holtz, F., and Lange, R. (2003) The influence of pressure and

629 composition on the viscosity of andesitic melts. Geochimica et Cosmochimica Acta, 67,
630 473-485.
631 Liebske, C., Schmickler, B., Terasaki, H., Poe, B., Suzuki, A., Funakoshi, K., Ando, R., and
632 Rubie, D. (2005) Viscosity of peridotite liquid up to 13 GPa: Implications for magma
633 ocean viscosities. Earth and Planetary Science Letters, 240, 589-604.
634 Mahon, K. I., Harr isson, T. M., and Drew, D. A., 1988. Ascent of a granitoid diapir in a
635 temperature varying medium. Journal of Geophysical Research. 94, 1174-1188.
636 Malfait, W.J., and Sanchez-Valle, C. (2013) Effect of water and network connectivity on
637 glass elasticity and melt fragility. Chemical Geology, 346, 72-80.
638 Mastin, L.G. (2002) Insights into volcanic conduit flow from an open-source numerical model.
639 Geochemistry, Geophysics, Geosystems, 3, 1029-1046.
640 Mastin, L.G. (2005) The controlling effect of viscous dissipation on magma flow in silicic
641 conduits. Journal of Volcanology and Geothermal Research, 143, 17-28.
642 Mastin, L.G., and Ghiorso, M.S. (2000) A numerical program for steady-state flow of
643 magma-gas mixtures through vertical eruptive conduits, USGS Open-File Report 00-209.
644 *U.S.* Geological Survey, Vancouver, WA, 56 pp.
645 Morizet, Y., Nichols, A. R. L., Kohn, S. C., Brooker, R. A., and Dingwell, D. B. (2007) The
646 influence of H_2O and CO_2 on the glass transition temperature: insights into the effects of
647 volatiles on magma viscosity. European Journal of Mineralogy, 19, 657-669.
648 Moynihan, C.T. (1995) Structural relaxation and the glass transition. Reviews in Mineralogy
649 and Geochemistry, 32, 1-19.
650 Misiti, V., Freda, C., Taddeucci, J., Romano, C., Scarlato, P., Longo, A., Papale, P., and Poe, B.

651 T. (2006) The effect of H_2O on the viscosity of K-trachytic melts at magmatic
652 temperatures. Chemical Geology, 235, 124-137.
653 Misiti, V., Vetere, F., Freda, C., Scarlato, P., Behrens, H., Mangiacapra, A., and Dingwell, D.
654 B. (2011) A general viscosity model of Campi Flegrei (Italy) melts. Chemical Geology,
655 290, 50-59.
656 Mori, S., Ohtani, E., and Suzuki, A. (2000) Viscosity of the albite melt to 7 GPa at 2000 K.
657 Earth and Planetary Science Letters, 175, 87-92.
658 Moore, G., Righter, K., and Carmichael, I.S.E. (1995) The effect of dissolved water on the
659 oxidation state of iron in natural silicate liquids. Contributions to Mineralogy and
660 Petrology, 120, 170-179.
661 Moretti, R. (2005) Polymerisation, basicity, oxidation state and their role in ionic modelling of
662 silicate melts. Annals of Geophysics, 48, 583-608
663 Mysen, B., Virgo, D., and Scarfe, C. (1980) Relations between the anionic structure and
664 viscosity of silicate melts-a Raman spectroscopic study. American Mineralogist, 65,
665 690–710.
666 Mysen, B., Virgo, D., Scarfe, C., and Cronin, D. (1985) Viscosity and structure of iron-and
667 aluminum-bearing calcium silicate melts at 1 atm. American Mineralogist, 70, 487-498.
668 Mysen, B.O. (1988) Structure and Properties of Silicate melts. Elsevier, Amesterdam, 1988,
669 354 pp.
670 Mysen, B.O., and Richet, P. (2005) Developments in Geochemistry 10, Silicate Glasses and
671 Melts Properties and Structure. Elsevier, Amsterdam.
672 Mysen, B.O., and Virgo, D. (1989) Redox equilibria, structure and properties of Fe-bearing

673 alumosilicate melts: relationship among temperature, composition and oxygen fugacity
674 in the system Na_2O-Al_2O_3-SiO_2-Fe-O. American Mineralogist, 74, 58-76.
675 Neuville, D., Courtial, P., Dingwell, D., and Richet, P. (1993) Thermodynamic and rheological
676 properties of rhyolite and andesite melts. Contributions to Mineralogy and Petrology, 113,
677 572-581.
678 O'Neill, H.S.C. (1987) Free energies of formation of NiO, CoO, Ni_2SiO_4, and Co_2SiO_4.
679 American Mineralogist, 72(3), 280-291.
680 Ottonello, G., Moretti, R., Marini, L., and Vetuschi Zuccolini, M. (2001) Oxidation state of
681 iron in silicate glasses and melts: a thermochemical model. Chemical Geology, 174(1-3),
682 157-179.
683 Papale, P. (1999) Modeling of the solubility of a two-component H_2O+CO_2 fluid in silicate
684 liquids. American Mineralogist, 84, 477-492.
685 Persikov, Y.S., Zharikov, V.A., Bukhtiyarov, P.G., and Pol'skoy, S.F. (1990) The effect of
686 volatiles on the properties of magmatic melts. European Journal of Mineralogy, 2(5),
687 621-642.
688 Persikov, E. (1991) The viscosity of magmatic liquids: experiment, generalized patterns. A
689 model for calculation and prediction. Applications. Advance in Physical Geochemistry, 9,
690 1-40.
691 Plazek, D.J., and Ngai, K.L. (1991) Correlation of polymer segmental chain dynamics with
692 temperature-dependent time-scale shifts. Macromolecules, 24, 1222-1224.
693 Press, W.M., Teukolski, S.A., Vetterling, W.T., and Flannery, B.P. (1992) Numerical recipes in
694 FORTRAN-The art of scientific computing, second edition, 963 p**.** Cambridge

University Press Cambridge, U.K.

Richet, P., Lejeune, A., Holtz, F., and Roux, J. (1996) Water and the viscosity of andesite melts. Chemical Geology, 128, 185-197.

Romano, C., Giordano, D., Papale, P., Mincione, V., Dingwell, D.B., and Rosi, M. (2003) The dry and hydrous viscosities of alkaline melts from Vesuvius and Phlegrean Fields. Chemical Geology, 202, 23-38.

Russell, J., Giordano, D., and Dingwell, D. (2003) High-temperature limits on viscosity of non-Arrhenian silicate melts. American Mineralogist, 88, 1390-1394.

Sato, H., Fugii, T., and Nakada, S. (1992) Crumbling of dacite dome lave and generation of pyroclastic flows at Unzen volcano. Nature, 360, 664-666.

Scarfe, C., Mysen, B., and Virgo, D. (1979) Changes in viscosity and density of melts of sodium disilicate, sodium metasilicate, and diopside composition with pressure. Year Book Carnegie Institute Washington, 78, 547–551.

Scarfe, C.M., Mysen, B.O., and Virgo, D. (1987) Pressure dependence of the viscosity of silicate melts. Magmatic processes: Physicochemical principles, 1, 59-67.

Scaillet, B., Holtz, F., Pichavant, M., and Schmidt, M. (1996) Viscosity of Himalayan leucogranites: Implications for mechanisms of granitic magma ascent. Journal of Geophysical Research, 101, 27691-27699.

Schulze, F., Behrens, H., Holtz, F., Rous, J., and Johannes, W. (1996) The influence of H_2O on the viscosity of a haplogranitic melt. American Mineralogist, 81, 1155-1165.

Schulze, F., Behrens, H., and Hurkuck, W. (1999) Determination of the influence of pressure and dissolved water on the viscosity of highly viscous melts; application of a new

parallel-plate viscometer. American Mineralogist, 84, 1512-1520.

Shaw, H. (1963) Obsidian-H_2O viscosities at 1000 and 2000 bars in the temperature range 700 to 900 °C. Journal of Geophysical Research, 68, 6337-6343.

Shaw, H.R. (1972) Viscosities of magmatic silicate liquids; an empirical method of prediction. American Journal of Science, 272, 870-893.

Silver, L. and Stolper, E. (1989) Water in albitic glasses. Journal of Petrology, 30, 667.

Silver, L. A., Ihinger, P. D., and Stolper, E. (1990) The influence of bulk composition on the speciation of water in silicate glasses. Contributions to Mineralogy and Petrology, 104, 142-162.

Stevenson, R., Bagdassarov, N., Dingwell, D., and Romano, C. (1998) The influence of trace amounts of water on the viscosity of rhyolites. Bulletin of Volcanology. 60, 89-97.

Stevenson, R.J., Dingwell, D.B., Webb, S.L., and Bagdassarov, N. S. (1995) The equivalence of enthalpy and shear stress relaxation in rhyolitic obsidians and quantification of the liquid-glass transition in volcanic processes. Journal of Volcanology and Geochermal Research, 68, 297-306.

Stevenson, R.J., Dingwell, D.B., Webb, S.L., and Sharp, T.G. (1996) Viscosity of microlite-bearing rhyolitic obsidians: an experimental study. Bulletin of Volcanology, 58, 298-309.

Stolper, E. (1982) The speciation of water in silicate melts. Geochimica et Cosmochimica Acta, 46, 2609-2620.

Tammann, G., and Hesse, W. (1926) Die abhängigkeit der viskosität von der temperature bei unterkühlten flüssigkeiten. Z Anorg Allg Chem, 156, 245-257.

739 Toplis, M., Dingwell, D., Hess, K., and Lenci, T. (1997) Viscosity, fragility, and
740 configurational entropy of melts along the join SiO_2-$NaAlSiO_4$. American Mineralogist,
741 82, 979-990.
742 Toplis, M.J., and Dingwell, D.B. (1996) The variable influence of P_2O_5 on the viscosity of
743 melts of differing alkali/aluminium ratio: Implications for the structural role of
744 phosphorus in silicate melts. Geochimica et Cosmochimica Acta, 60(21), 4107-4121.
745 Toplis, M.J., Dingwell, D.B., and Libourel, G. (1994) The effect of phosphorus on the iron
746 redox ratio, viscosity, and density of an evolved ferro-basalt. Contributions to
747 Mineralogy and Petrology, 117, 293-304.
748 Vetere, F., Behrens, H., Holtz, F., and Neuville, D. (2006) Viscosity of andesitic melts-new
749 experimental data and a revised calculation model. Chemical Geology, 228, 233-245.
750 Vetere, F., Behrens, H., Misiti, V., Ventura, G., Holtz, F., De Rosa, R., and Deubener, J. (2007)
751 The viscosity of shoshonitic melts (Vulcanello Peninsula, Aeolian Islands, Italy): Insight
752 on the magma ascent in dikes. Chemical Geology, 245, 89-102.
753 Vetere, F., Behrens, H., Schuessler, J., Holtz, F., Misiti, V., and Borchers, L. (2008) Viscosity
754 of andesite melts and its implication for magma mixing prior to Unzen 1991-1995
755 eruption. Journal of Volcanology and Geochermal Research, 175, 208-217.
756 Vogel, D.H. (1921) Das Temperaturabh ngigkeitsgesetz der Viskosit t von Flüssigkeiten.
757 Physical.Z., 645-646.
758 Webb, S.L., and Dingwell, D.B. (1995) Viscoelasticity. Reviews in Mineralogy and
759 Geochemistry, 32, 95-119.
760 Whittington, A., Richet, P., and Holtz, F. (2000) Water and the viscosity of depolymerized

761 aluminosilicate melts. Geochimica et Cosmochimica Acta, 64, 3725-3736.
762 Whittington, A., Richet, P., Linard, Y., and Holtz, F. (2001) The viscosity of hydrous
763 phonolites and trachytes. Chemical Geology, 174, 209-223.
764 Zhang, Y. (1999) H_2O in rhyolitic glasses and melts: measurement, speciation, solubility, and
765 diffusion. Reviews of Geophysics, 37, 493-516.
766 Zhang, Y., Xu, Z., and Liu, Y. (2003) Viscosity of hydrous rhyolitic melts inferred from
767 kinetic experiments, and a new viscosity model. American Mineralogist, 88, 1741-1752.
768

Tables

Table 1 Experimental data of natural Fe-bearing melt viscosity used in this model (including data for calibration and for test)

Reference	Melt	T (K)	P (kbar)	H_2O (wt%)	N#
Giordano et al. (2003b)	Basalt	798-1004	0.00	0.02-1.5	22
Liebske et al. (2003)*	Andesite	1006-1098	0.00	0.00	22
Richet et al. (1996)	Andesite	996-1123	0.00	0.00	41
Toplis et al. (1994)	Basalt (MTV1)	1670-1673	0.00	0.00	4
	Basalt (MTV2)	1572-1867	0.00	0.00	4
	Basalt (MTV3)	1621-1769	0.00	0.00	4
	Basalt (MTV4)	1719-1867	0.00	0.00	4
	Basalt (MTV6)	1673-1873	0.00	0.00	4
	Basalt (MTV7)	1673-1873	0.00	0.00	3
	Basalt (MTV8)	1673-1873	0.00	0.00	3
	Basalt (MTV9)	1673-1873	0.00	0.00	3
Shaw (1963)	Rhyolite	973-1173	1.0-2	4.3-6.2	5
Persikov (1991)	Rhyolite	973-1173	0.5-7	2.1-12.3	12
Liebske et al. (2005)*	Peridotite	2043-2523	28-130	0.00	21
Vetere et al. (2007)*	Shoshonite	733-1573	0.001-5	0.019-4.75	21
Vetere et al. (2008)	Andesite	747-1573	3.0-10	0.02-6.31	27
Stevenson et al. (1995)	Rhyolite	897-965	0.00	0.16-0.21	6
Kushiro (1986)	Olivine Tholeiite I	1648-1748	7-12.5	0.00	6
	Olivine Tholeiite II	1623-1673	7-12.5	0.00	3
	Low-alkali Tholeiite	1623-1673	10.0-15	0.00	5
	Alkali Olivine Basalt	1623-1698	7.0-15	0-1.08	7
	K-rich Alkali Basalt	1673-1698	7-12.5	0.00	3

Number of measurements.

* The data are not used for the calibration of the model, but for the check.

777 **Table 2 Parameters for this model**

Parameters	Value
a	-4.753468E+00 (1.116472E-01)
b_1	7.317415E+03 (3.356892E-01)
b_2	-1.572090E+02 (3.719342E-02)
b_3	-3.068000E-02 (3.740712E-03)
b_4	1.816191E-01 (6.108900E-02)
b_5	2.185230E-01 (4.804092E-02)
c_1	1.672632E+02 (3.729234E-01)
c_2	-1.765680E+01 (1.779570E+00)
c_3	-6.101450E-05 (3.555688E-05)
c_4	3.044336E-04 (1.376224E-04)
c_5	6.653222E-04(3.630155E-05)

778

779 The parameters and standard deviations (in parentheses) are estimated by

780 Levenberg-Marquardt method of nonlinear least squares according to Press et al. (1992)

781

Table 3 Comparison between the predictions of models for melt viscosity and the experimental data with known redox states

Model		N[i]	Various[a]	Basalt[b]	Shoshonite[c]	Andesite[d]	Rhyolite[e]	Ref[j]
This model	RMSE[f]	11	0.23	0.26	0.40	0.16	0.32	This study
S-B-W model	RMSE	8	0.77	0.99		0.15		1, 2
H-Z model	RMSE	37	0.70[g]	0.35[g]	1.55	0.79[g]	0.32	3
G-R-D model	RMSE	18	0.68[h]	0.56	0.62	0.77[h]	0.99	4
Baker model	RMSE	7					0.54	5
S-B-H model	RMSE	5					1.20	6
H-D model	RMSE	6					0.72	7
Z-X-L model	RMSE	7					2.03	8
A-G-S model	RMSE	6					2.53	9
H-Z-X model	RMSE	11					2.03	10
R-L-H model	RMSE	10				0.89		11
V-B-S model	RMSE	7				0.16		12, 13
V-B-M model	RMSE	6			0.17			14
M-V-F model	RMSE	6			0.82			15, 16

Note: Blank range indicates the melt ranges where the specific models are not intended to be applied; the *T-P-X* range of each model is shown in the text in detail

[a] The viscosity calculated for various melts in the stated *T-P-X* range of relevant models

[b] The viscosity calculated for basaltic melts in the stated *T-P-X* range of relevant models

[c] The viscosity calculated for shoshonitic melts in the stated *T-P-X* range of relevant models

[d] The viscosity calculated for andesitic melts in the stated *T-P-X* range of relevant models

[e] The viscosity calculated for rhyolitic melts in the stated *T-P-X* range of relevant models

[f] The root-mean-square-error (log units) between the measured and calculated data defined in Eqn. (1) in the Text.

[g] The experimental data belong to the outliers of H-Z model are not in comparison here (see the Text for detail)

[h] The experimental data belong to the outliers of G-R-D model are not compared here (see the Text for detail)

i The number of parameters used in each model

[j] The reference number: 1, Shaw (1972); 2, Bottinga and Weill (1972); 3, Hui and Zhang (2007); 4, Giordano et al. (2008); 5, Baker (1996); 6, Schulze et al. (1996); 7, Hess and Dingwell (1996); 8, Zhang et al. (2003); 9, Ardia et al. (2008); 10, Hui et al. (2009); 11, Richet et al. (1996); 12, Vetere et al. (2006); 13, Vetere et al. (2008); 14, Vetere et al. (2007); 15, Misiti et al. (2006); 16, Misiti et al. (2011)

Figure Captions

Fig. 1. The melt compositions of the database in this study. (a) Total alkalis (Na_2O+K_2O, wt%) versus SiO_2 (wt%) diagram (Le Bas et al., 1986). F, foidite; Ph, phonolite; Pc, picrobasalt; B, basalt; R, rhyolite ; T, trachyte or trachydacite; H1, basanite or tephrite; H2, phonotephrite; H3, tephriphonolite; J1, trachybasalt; J2, basaltic trachyandesite; J3, trachyandesite; L1, basaltic andesite; L2, andesite ; L3, dacite. (b) Total iron content (FeO_{tot}, wt%) versus SiO_2 (wt%) diagram.

Fig. 2. Comparisons of the calculated data by general models (e.g., this model; H-Z model; G-R-D model) with experimental viscosity data, including those with known (Data_redox_state_known) and unknown redox states (Data_redox_state_unknown). Note: only the experimental data within the stated *T-P-X* ranges of models are used. Since the H-Z and G-R-D models intended to predict the viscosity at the atmospheric pressure, the data beyond their pressure range are not used in Fig 2 (b-c). The circles denote the experimental data with known redox states, which include those used for calibration of the model (filled circles), and the ones used only for testing the predictability of the model (open circles). In addition, the filled squares are the experimental data with unknown redox states. The dashed lines indicate 95% confidence level of the calculated viscosities. RMSE is the abbreviation of root-mean-square-error (log units) between the measured and calculated data. (a) Comparison between the calculated data with this model and the experimental data. Note: in this figure, the FeO and Fe_2O_3 contents were arbitrarily calculated, assuming that half of the total iron FeO_{tot} (wt%) is FeO (wt%) and the other half is Fe_2O_3 (wt%). (b) Comparison between the calculated data with H-Z model and the experimental data. Note: the outliers of H-Z model

(Toplis et al., 1994; Richet et al., 1996) are not plotted. (c) Comparison between the calculated data with G-R-D model and the experimental data. Note: the outliers of G-R-D model (Richet et al., 1996) are not plotted. The sources of experimental data with known redox states (Data_redox_state_known): Shaw (1963); Kushiro (1986); Persikov (1991); Toplis et al. (1994); Stevenson et al. (1995); Richet et al. (1996); Giordano et al. (2003b); Liebske et al. (2003, 2005) ; Vetere et al. (2007, 2008). Note: most of these data are used in the model calibration, except those data (Liebske et al., 2003, 2005; Vetere et al., 2007) that are not used for parameterization, but for checking the predictability of this model. The sources of experimental data with unknown redox states (Data_redox_state_unknown): Neuville et al. (1993); Stevenson et al. (1996); Alidibirov et al.(1997); Gottsman et al. (2002); Roman et al. (2003); Misiti et al. (2006) ; Misiti et al. (2011).

Fig. 3. Comparison between the calculated data with this model and the experimental data with known redox states (Data_redox_state_known). The circles denote the experimental data with known redox states, which include the ones used for the calibration of the model (filled circles), and the ones used for testing the predictability of the model (open circles). The dashed lines indicate 95% confidence level of the calculated viscosities. RMSE is the abbreviation of root-mean-square-error (log units) between the measured and calculated data. In this case, the experimental measurements of iron oxidation state are taken as inputs for calculation of melt viscosity. The experimental data sources are the same as those defined in Fig. 2.

Fig. 4. The prediction of this model in the high pressure range ($P \geqq 1$kbar). The symbols are the experimental measurements of melt viscosity. The dashed lines indicate 95% confidence

level of the calculated viscosities.

Fig. 5. The pressure dependence of viscosity for Fe-bearing andesitic melts with different H_2O contents. The source of the melts: Vetere et al. (2008).

Fig. 6. The effect of redox state on viscosity of various melts at 0.001 kbar and 1473 K. (a) The viscosity of various melts varying with Fe^{3+}/Fe_{tot}; (b) The viscosity of various melts varying with oxygen fugacity; (c) The 'network modifers' parameter (VSM) varying with oxygen fugacity. See the Text for detail. The melt source: basalt, Giordano et al. (2003b); andesite, Liebske et al. (2003); rhyolite, Persikov (1991).

Fig. 7. The properties of silicate melts predicted by this model. (a) Computed values of Tg (K) vs. H_2O content (wt%) for diverse melt compositions including: alkali basalt, theoleiite, shoshonite, andesite, rhyolite, assuming q (cooling rate) as 0.0833 K/s. (b) Model curves for the values of fragility (m) vs. H_2O content (wt%) for the same melts as shown in Fig.7a , assuming q (cooling rate) as 0.0833 K/s. Explosive volcanic behavior is favored by melt with low fragility (e.g., strong) at high volatile contents.

Figures

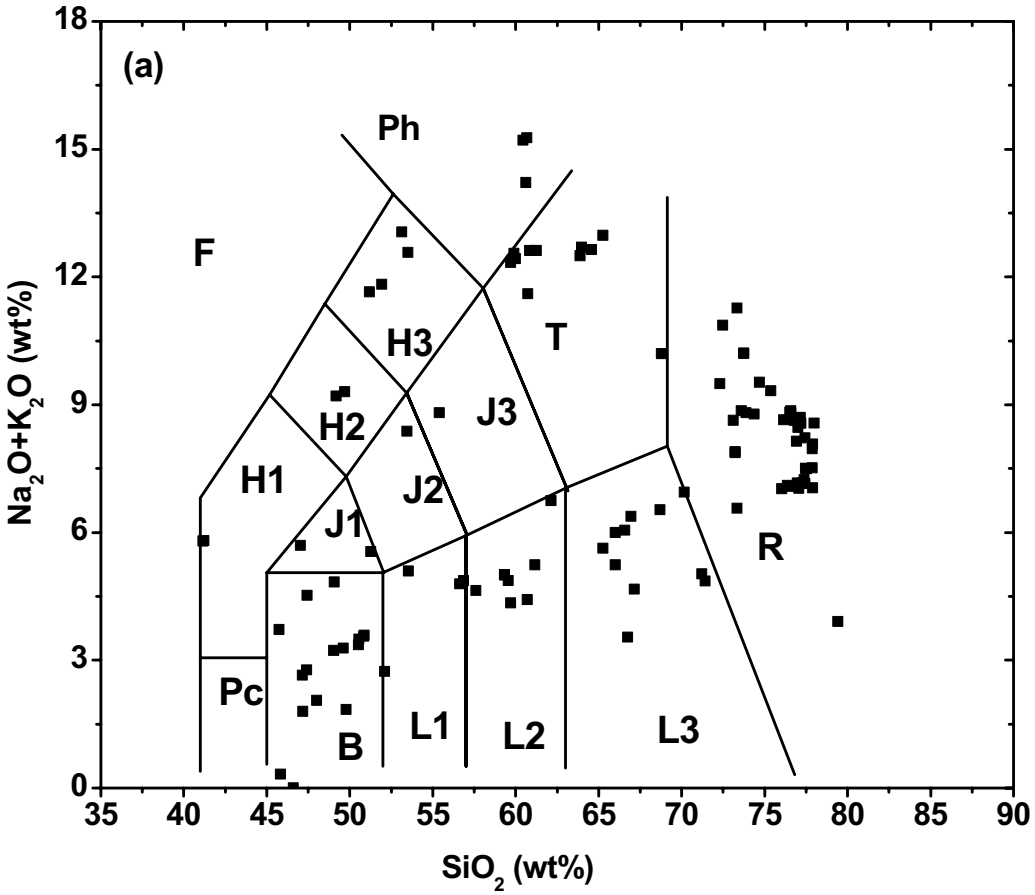

Fig.1a

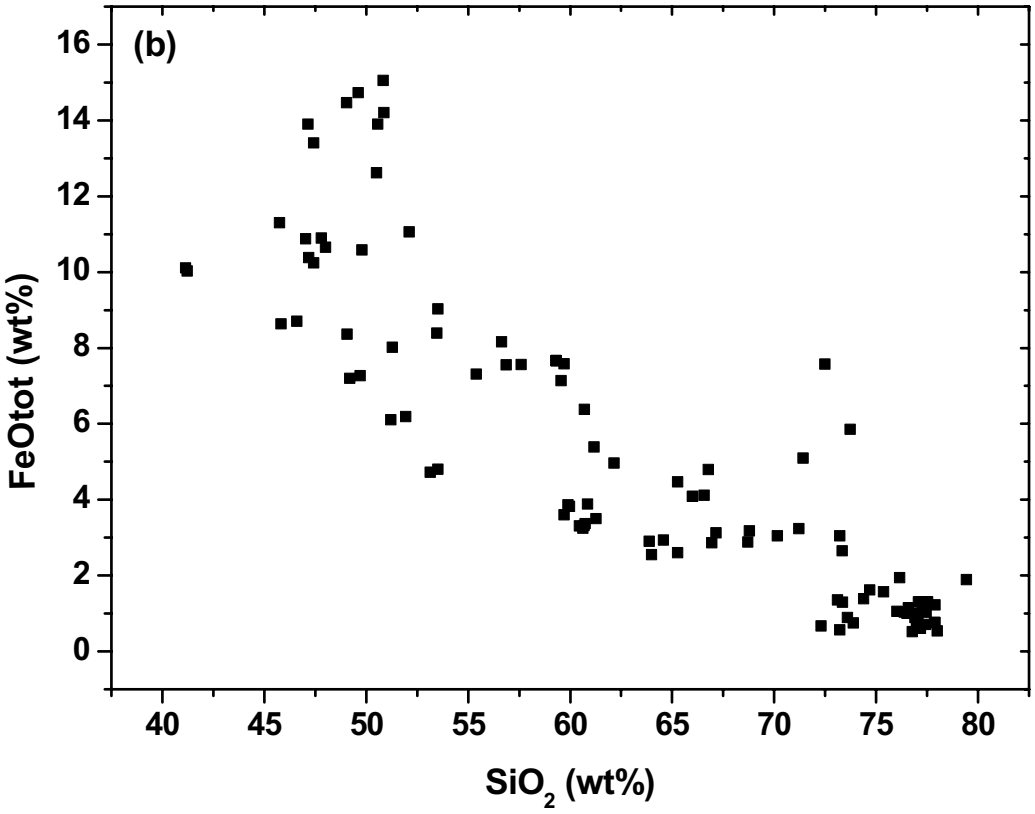

Fig. 1b

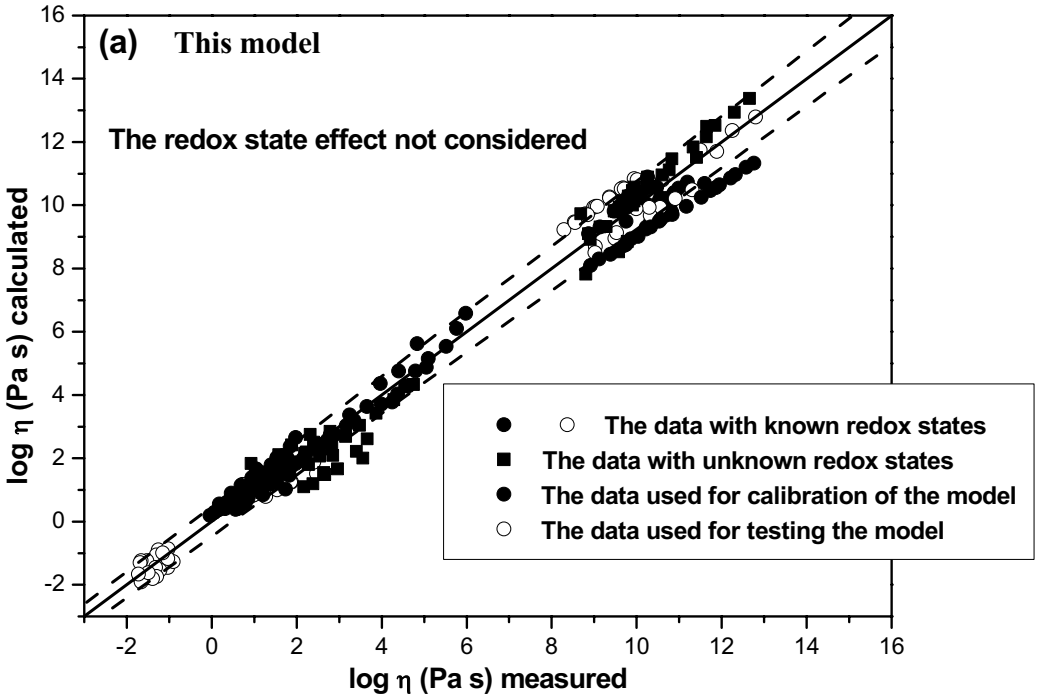
(a) This model
The redox state effect not considered
log η (Pa s) calculated
log η (Pa s) measured
The data with known redox states
The data with unknown redox states
The data used for calibration of the model
The data used for testing the model

Fig. 2a

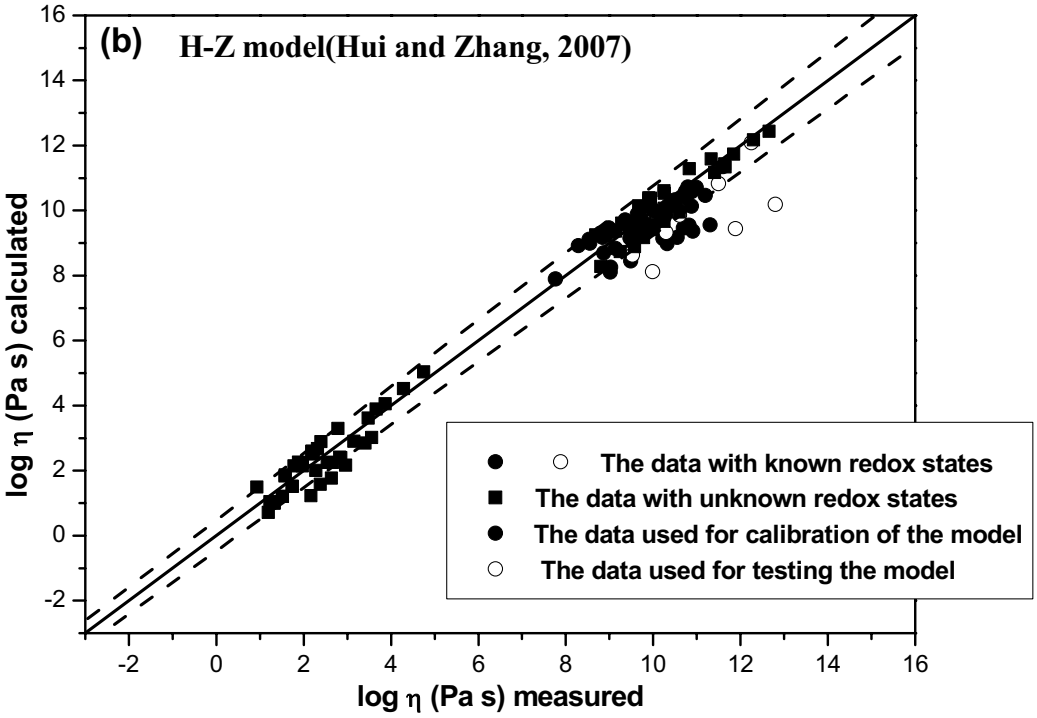
(b)
H-Z model(Hui and Zhang, 2007)
log η (Pa s) calculated
log η (Pa s) measured
The data with known redox states
The data with unknown redox states
The data used for calibration of the model
The data used for testing the model

Fig. 2b

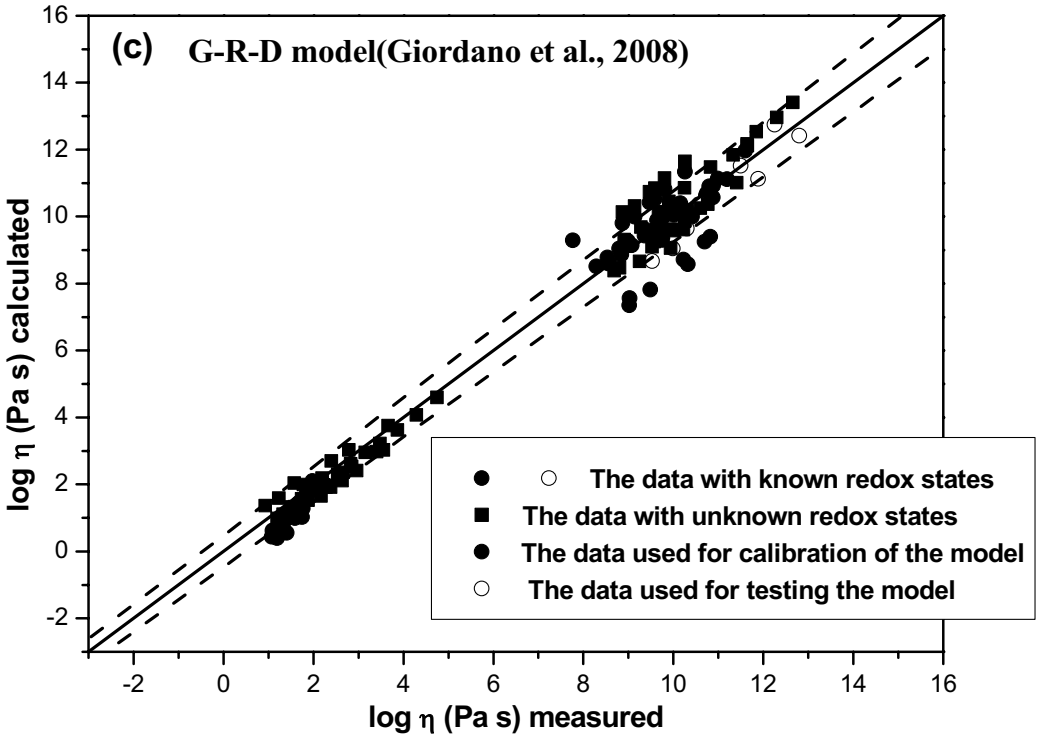
(c) G-R-D model(Giordano et al., 2008)
log η (Pa s) calculated
log η (Pa s) measured
The data with known redox states
The data with unknown redox states
The data used for calibration of the model
The data used for testing the model

Fig. 2c

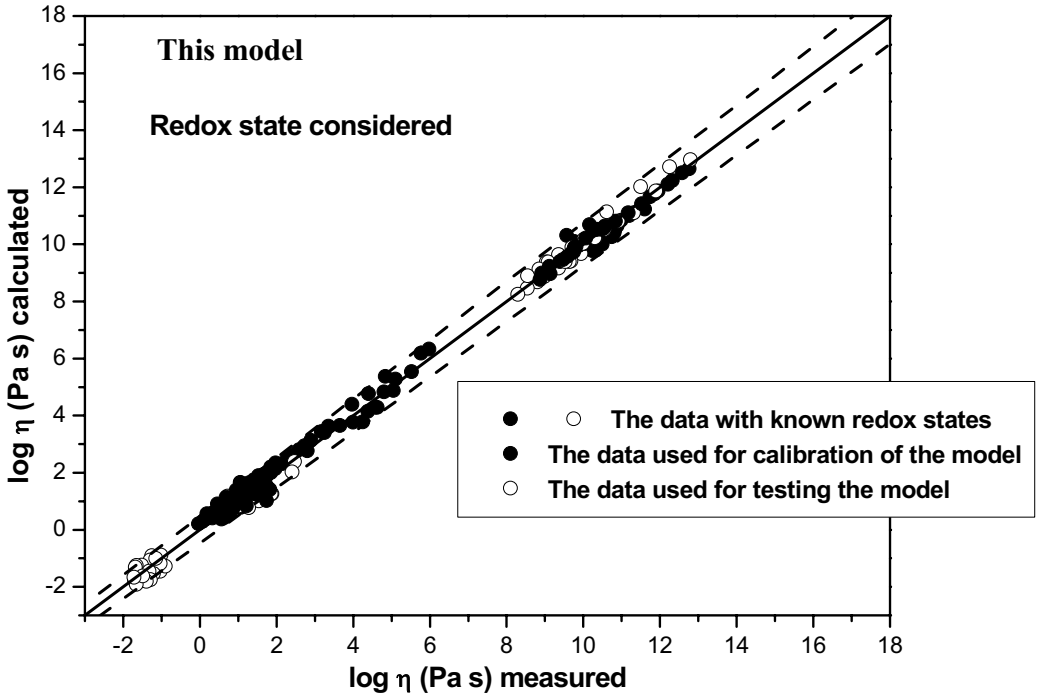
This model
Redox state considered
log η (Pa s) calculated
log η (Pa s) measured
The data with known redox states
The data used for calibration of the model
The data used for testing the model
18
16
14
12
10
8
6
4
2
0
-2
-2
0
2
4
6
8
10
12
14
16
18

Fig. 3

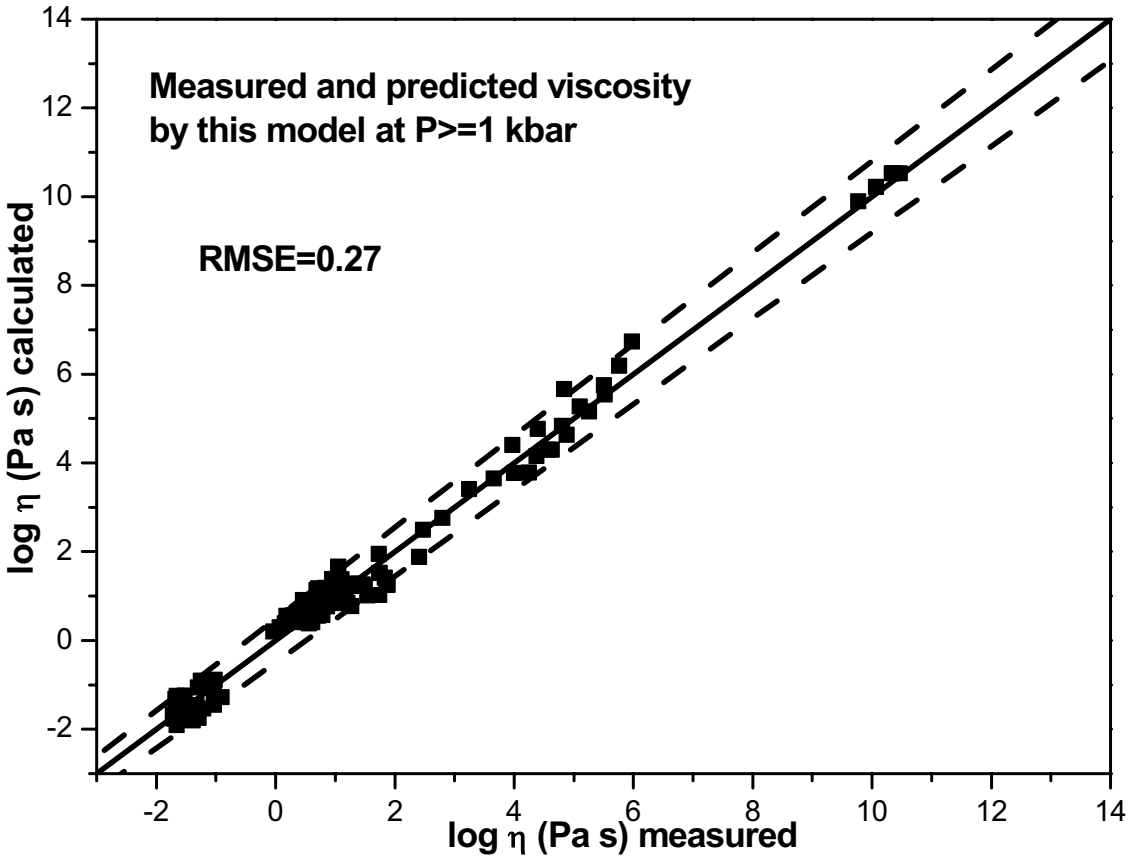
Measured and predicted viscosity
by this model at P>=1 kbar
RMSE=0.27
log η (Pa s) calculated
log η (Pa s) measured
14
12
10
8
6
4
2
0
-2
-2
0
2
4
6
8
10
12
14

Fig.4

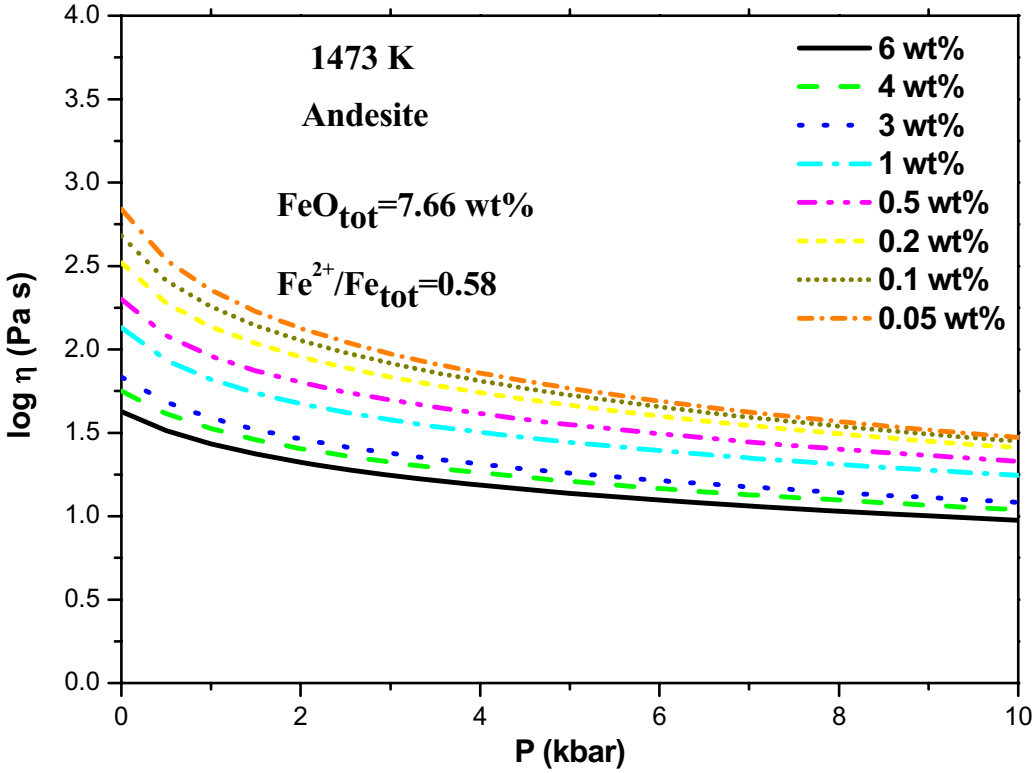
1473 K
Andesite
FeO$_{tot}$=7.66 wt%
Fe^{2+}/Fe$_{tot}$=0.58
6 wt%
4 wt%
3 wt%
1 wt%
0.5 wt%
0.2 wt%
0.1 wt%
0.05 wt%
log η (Pa s)
P (kbar)
0.0
0.5
1.0
1.5
2.0
2.5
3.0
3.5
4.0
0
2
4
6
8
10

Fig.5

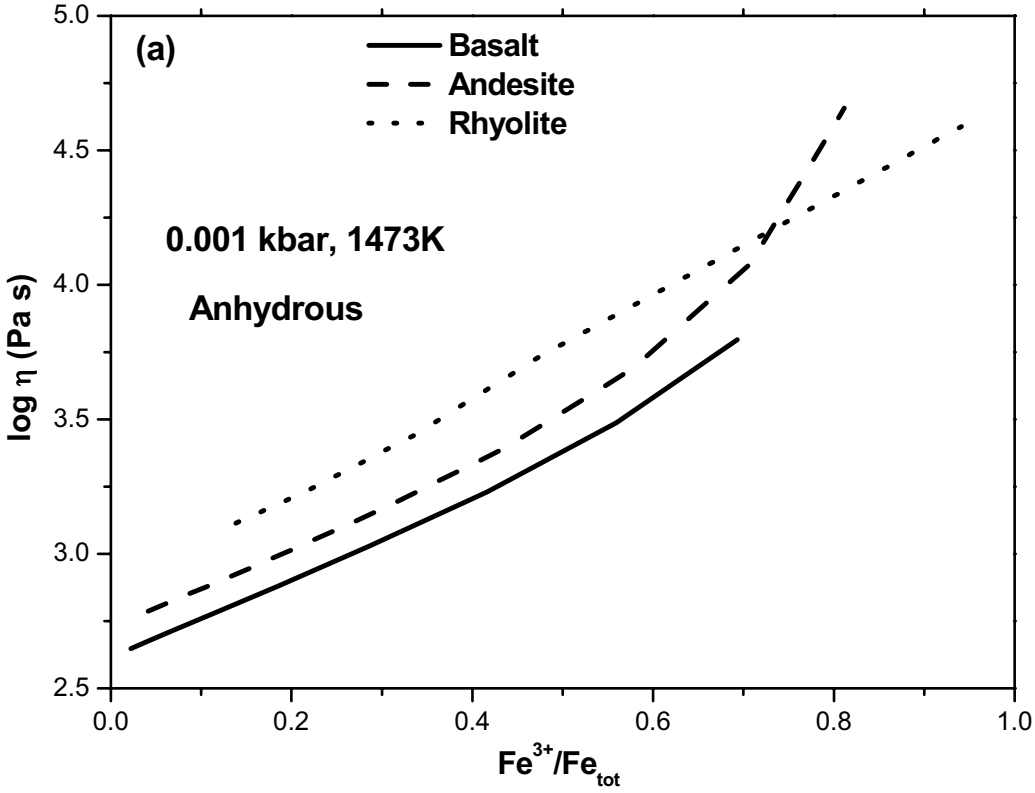
(a)
Basalt
Andesite
Rhyolite
0.001 kbar, 1473K
Anhydrous
log η (Pa s)
5.0
4.5
4.0
3.5
3.0
2.5
0.0
0.2
0.4
0.6
0.8
1.0
Fe3+/Fetot

Fig.6a

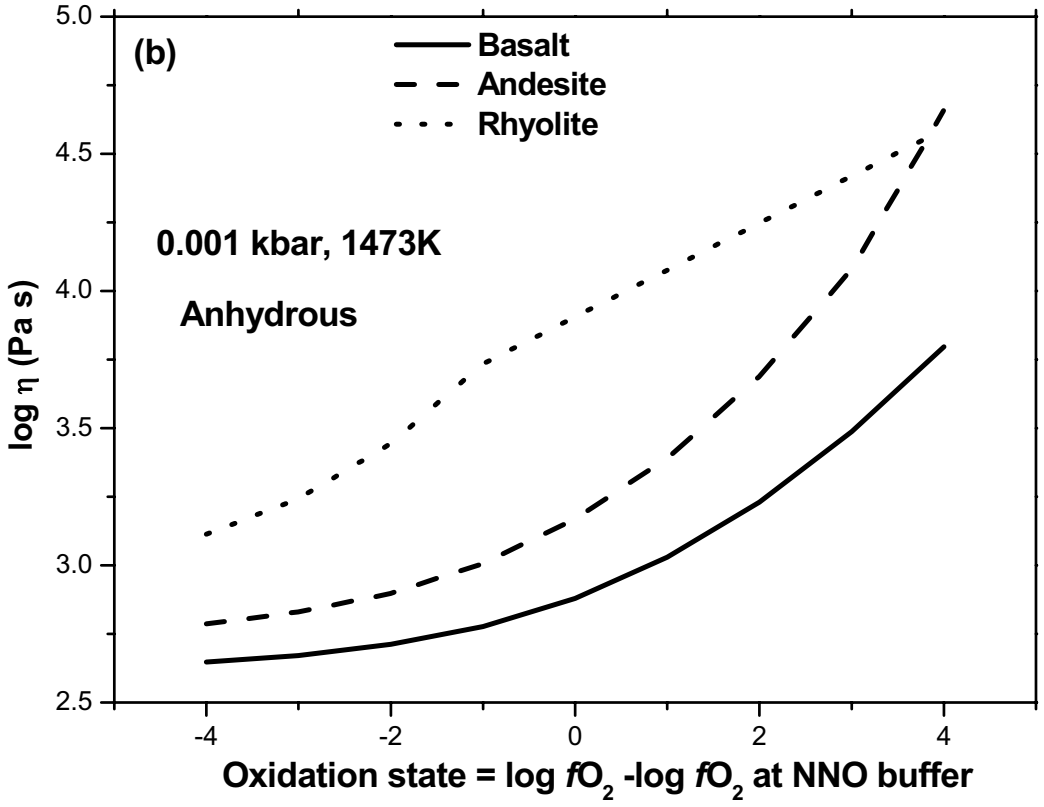
(b)
Basalt
Andesite
Rhyolite
0.001 kbar, 1473K
Anhydrous
log η (Pa s)
5.0
4.5
4.0
3.5
3.0
2.5
-4
-2
0
2
4
Oxidation state = log fO2 -log fO2 at NNO buffer

Fig. 6b

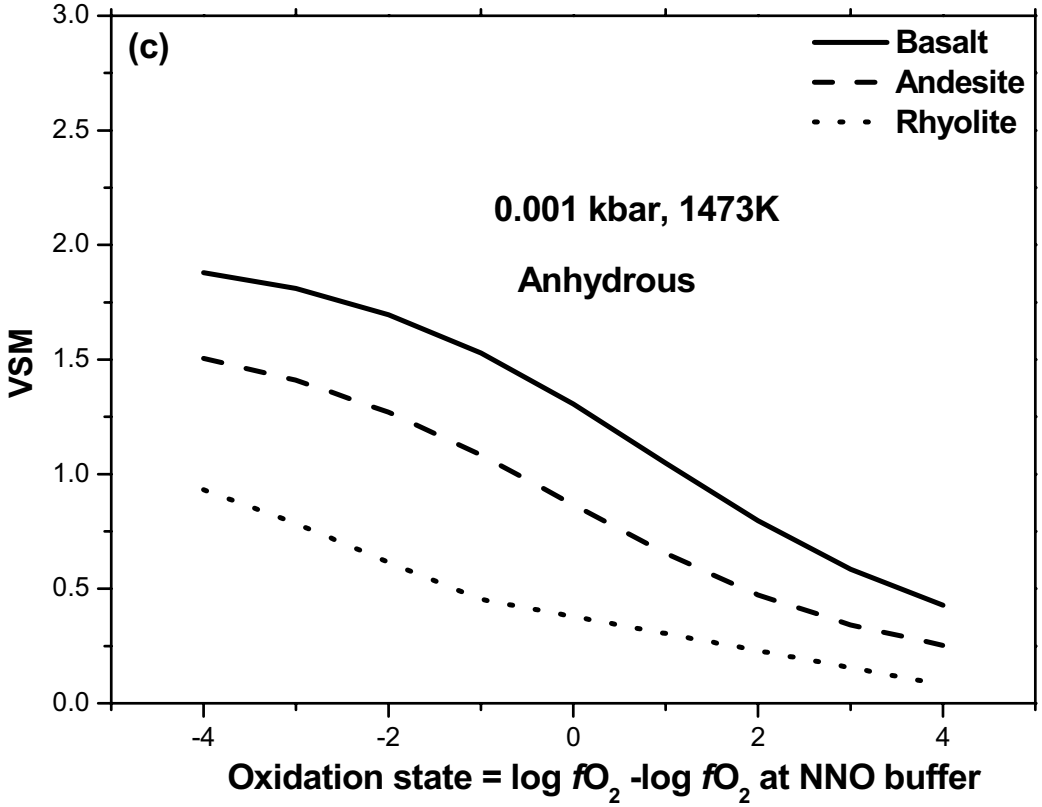
(c)
Basalt
Andesite
Rhyolite
0.001 kbar, 1473K
Anhydrous
VSM
3.0
2.5
2.0
1.5
1.0
0.5
0.0
-4
-2
0
2
4
Oxidation state = log fO2 -log fO2 at NNO buffer

Fig. 6c

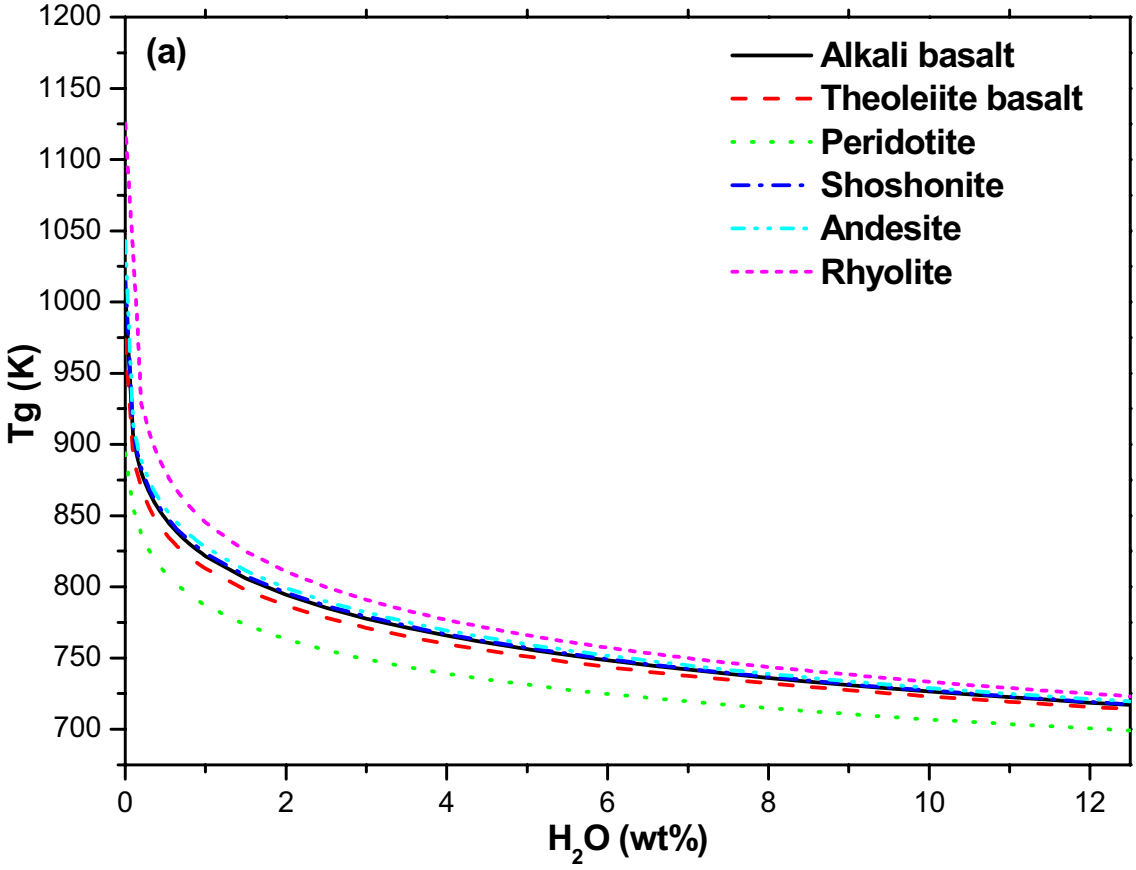
(a)
Alkali basalt
Theoleiite basalt
Peridotite
Shoshonite
Andesite
Rhyolite
Tg (K)
H2O (wt%)
1200
1150
1100
1050
1000
950
900
850
800
750
700
0
2
4
6
8
10
12

Fig.7a

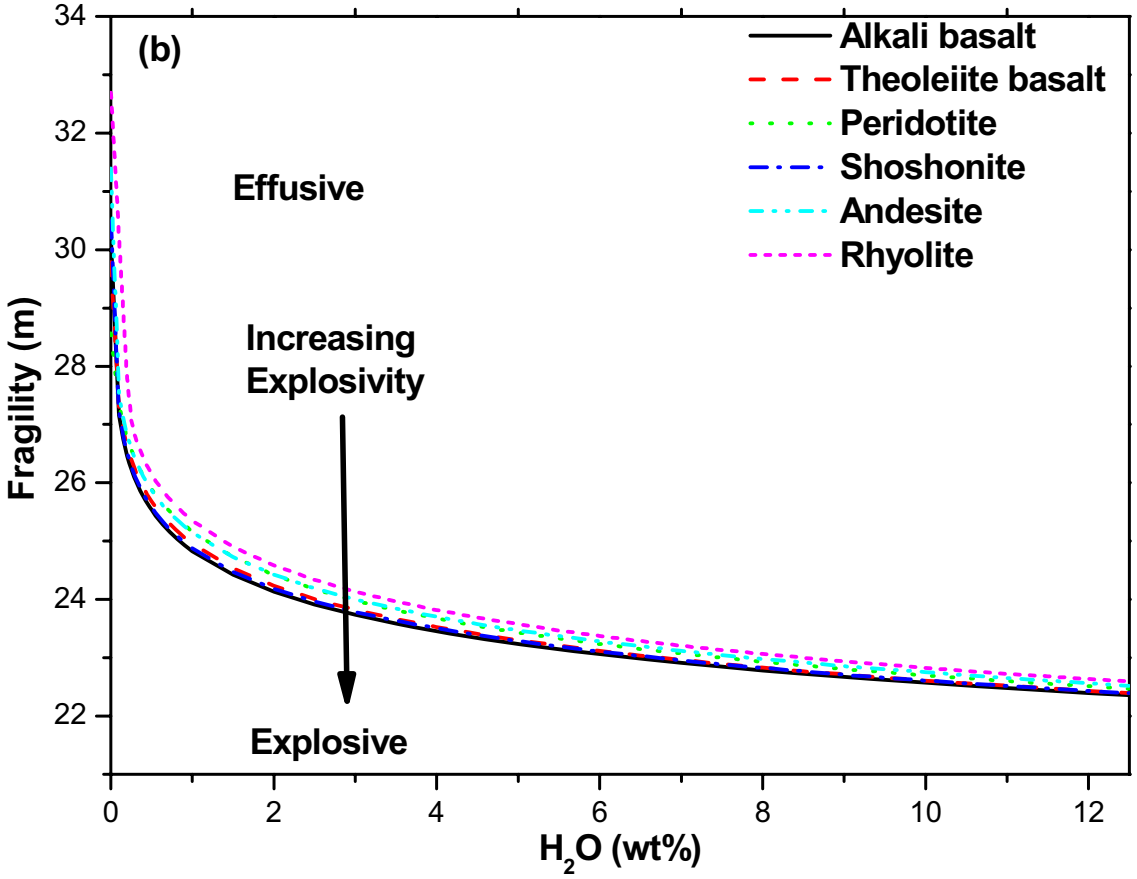
(b)
Alkali basalt
Theoleiite basalt
Peridotite
Shoshonite
Andesite
Rhyolite
Effusive
Increasing
Explosivity
Explosive
Fragility (m)
H2O (wt%)
34
32
30
28
26
24
22
0
2
4
6
8
10
12

Fig. 7b